INFERENCE OF CELL TYPE COMPOSITION FROM HUMAN BRAIN TRANSCRIPTOMIC DATASETS ILLUMINATES THE EFFECTS OF AGE, MANNER OF DEATH, DISSECTION, AND PSYCHIATRIC DIAGNOSIS

*Megan Hastings Hagenauer, Ph.D.[1], Anton Schulmann, M.D.[2], Jun Z. Li, Ph.D.[3], Marquis P. Vawter, Ph.D.[4], David M. Walsh, Psy.D.[4], Robert C. Thompson, Ph.D.[1], Cortney A. Turner, Ph.D.[1], William E. Bunney, M.D.[4], Richard M. Myers, Ph.D.[5], Jack D. Barchas, M.D.[6], Alan F. Schatzberg, M.D.[7], Stanley J. Watson, M.D., Ph.D.[1], Huda Akil, Ph.D.[1]

[1]Mol. Behavioral Neurosci. Inst., Univ. of Michigan, Ann Arbor, MI, USA; [2] Janelia Research Campus, Howard Hughes Medical Institute, Ashburn, VA, USA, [3]Genet., Univ. of Michigan, Ann Arbor, MI, USA; [4]Univ. of California, Irvine, CA; [5]HudsonAlpha Inst. for Biotech., Huntsville, AL, USA; [6]Stanford, Palo Alto, CA, [7]Cornell, New York, NY, USA

*Corresponding Author: Megan Hastings Hagenauer, Ph.D.

e-mail: hagenaue@umich.edu

Molecular Behavioral Neuroscience Institute (MBNI)

205 Zina Pitcher Pl.

Ann Arbor, MI 48109

Abstract

Psychiatric illness is unlikely to arise from pathology occurring uniformly across all cell types in affected brain regions. Despite this, transcriptomic analyses of the human brain have typically been conducted using macro-dissected tissue due to the difficulty of performing single-cell type analyses with donated post-mortem brains. To address this issue statistically, we compiled a database of several thousand transcripts that were specifically-enriched in one of 10 primary cortical cell types in previous publications. Using this database, we predicted the relative cell type composition for 833 human cortical samples using microarray or RNA-Seq data from the Pritzker Consortium (GSE92538) or publicly-available databases (GSE53987, GSE21935, GSE21138, CommonMind Consortium). These predictions were generated by averaging normalized expression levels across transcripts specific to each cell type using our R-package *BrainInABlender* (validated and publicly-released: https://github.com/hagenaue/BrainInABlender). Using this method, we found that the principal components of variation in the datasets strongly correlated with the neuron to glia ratio of the samples. This variability was not simply due to dissection – the relative balance of brain cell types appeared to be influenced by a variety of demographic, pre- and post-mortem variables. Prolonged hypoxia around the time of death predicted increased astrocytic and endothelial gene expression, illustrating vascular upregulation. Aging was associated with decreased neuronal gene expression. Red blood cell gene expression was reduced in individuals who died following systemic blood loss. Subjects with Major Depressive Disorder had decreased astrocytic gene expression, mirroring previous morphometric observations. Subjects with Schizophrenia had reduced red blood cell gene expression, resembling the hypofrontality detected in fMRI experiments. Finally, in datasets containing samples with especially variable cell content, we found that controlling for predicted sample cell content while evaluating differential expression improved the detection of previously-identified psychiatric effects. We conclude that accounting for cell type can greatly improve the interpretability of transcriptomic data.

1. Introduction

The human brain is a remarkable mosaic of diverse cell types stratified into rolling cortical layers, arching white matter highways, and interlocking deep nuclei. In the past decade, we have come to recognize the importance of this cellular diversity in even the most basic neural circuits. At the same time, we have developed the capability to comprehensively measure the thousands of molecules essential for cell function. These insights have provided conflicting priorities within the study of psychiatric illness: do we carefully examine individual molecules within their cellular and anatomical context or do we extract transcript or protein en masse to perform large-scale unbiased transcriptomic or proteomic analyses? In rodent models, researchers have escaped this dilemma by a boon of new technology: single cell laser capture, cell culture, and cell-sorting techniques can provide sufficient extract for transcriptomic and proteomic analyses. However, single cell type analyses of the human brain are far more challenging (1–3) – live tissue is only available in the rarest of circumstances and intact single cells are difficult to dissociate from post-mortem tissue without intensive procedures like laser capture microscopy.

Therefore, to date, the vast majority of unbiased transcriptomic analyses of the human brain have been conducted using macro-dissected, cell-type heterogeneous tissue. On Gene Expression Omnibus (GEO) alone, there are at least 63* publicly-available macro-dissected post-mortem human brain tissue datasets, and many others are available to researchers via privately-funded portals (Stanley Medical Research Institute, Allen Brain Atlas, CommonMind Consortium). These datasets have provided us with novel hypotheses (e.g., (4,5)), but often a relatively small number of candidate molecules survive analysis despite careful sample collection, and interpreting molecular results in isolation from their respective cellular context can be exceedingly difficult. At the core of this issue is the inability to differentiate between (1) alterations in gene expression that reflect an overall disturbance in the relative ratio of the different cell types comprising the tissue sample, and (2) intrinsic dysregulation of one or more cell types, indicating perturbed biological function.

* As of 9-14-2017

In this manuscript, we present results from an easily accessible solution to this problem that allows researchers to statistically estimate the relative number or transcriptional activity of particular cell types in macro-dissected human brain transcriptomic data by tracking the collective rise and fall of previously identified cell type specific transcripts. Similar techniques have been used to successfully predict cell type content in human blood samples (6–9), as well as diseased and aged brain samples (10–12). Our method was specifically designed for application to large, highly-normalized human brain transcriptional profiling datasets, such as those commonly used by neuroscientific research bodies such as the Pritzker Neuropsychiatric Research Consortium and the Allen Brain Institute.

We took advantage of a series of newly available data sources depicting the transcriptome of known cell types, and applied them to infer the relative balance of cell types in our tissue samples. We draw from seven large studies detailing cell-type specific gene expression in a wide variety of cells in the forebrain and cortex (2,13–18). Our analyses include all major categories of cortical cell types (17), including two overarching categories of neurons that have been implicated in psychiatric illness (19): projection neurons, which are large, pyramidal, and predominantly excitatory, and interneurons, which are small and predominantly inhibitory (20). These are accompanied by three prevalent forms of glia that make up the majority of cells in the brain: oligodendrocytes, which provide the insulating myelin sheath for axons (21), astrocytes, which help create the blood-brain barrier and provide structural and metabolic support for neurons (21), and microglia, which serve as the brain's resident macrophages and provide an active immune response (21). We also incorporate vascular cell types: endothelial cells, which line the interior surface of blood vessels, and mural cells (smooth muscle cells and pericytes), which regulate blood flow (22). We included progenitor cells because they are widely implicated in the pathogenesis of mood disorders (23). Within the cortex, these cells mostly take the form of immature oligodendrocytes (17). Finally, the primary cells found in blood, erythrocytes or red blood cells (RBCs), carry essential oxygen throughout the brain. These cells lack a cell nucleus and do not generate new RNA, but still contain an existing, highly-specialized transcriptome (24). The relative presence of these cells could

arguably represent overall blood flow, the functional marker of regional neural activity traditionally used in human imaging studies.

To characterize the balance of these cell types in psychiatric samples, we first demonstrate that our method of summarizing cell type specific gene expression into a single metric ("cell type index") can reliably predict relative cell type balance in a variety of validation datasets. Then we discover that the predicted cell type balance of samples can explain a large percentage of the variation in macro-dissected human brain microarray and RNA-Seq datasets. This variability is driven by pre- and post-mortem subject variables, such as age, aerobic environment, and large scale blood loss, in addition to dissection. Finally, we demonstrate that our method enhances our ability to discover and interpret psychiatric effects in human transcriptomic datasets, uncovering previously-documented changes in cell type balance in relationship to Major Depressive Disorder and Schizophrenia and potentially increasing our sensitivity to detect genes with previously-identified relationships to Bipolar Disorder and Schizophrenia in datasets that contain samples with highly-variable cell content.

2. Methods

2.1 Compiling a Database of Cell Type Specific Transcripts

To perform this analysis, we compiled a database of several thousand transcripts that were specifically-enriched in one of nine primary brain cell types within seven published single-cell or purified cell type transcriptomic experiments using mammalian brain tissues (2,13–18). These primary brain cell types included six types of support cells: astrocytes, endothelial cells, mural cells, microglia, immature and mature oligodendrocytes, as well as two broad categories of neurons (interneurons and projection neurons). We also included a category for neurons that were extracted without purification by subtype ("neuron_all"). The experimental and statistical methods for determining whether a transcript was enriched in a particular cell type varied by publication (**Table 1**), and included both RNA-Seq and

microarray datasets. We focused on cell-type specific transcripts identified using cortical or forebrain samples because the data available for these brain regions was more plentiful than for the deep nuclei or the cerebellum. In addition, we artificially generated a list of 17 transcripts specific to erythrocytes by searching Gene Card for erythrocyte and hemoglobin-related genes (http://www.genecards.org/).

In all, we curated gene expression signatures for 10 cell types expected to account for most of the cells in the cortex. Our final database included 2499 unique human-derived or orthologous (as predicted by HCOP using 11 available databases: http://www.genenames.org/cgi-bin/hcop) transcripts, with a focus on coding varieties. We have made this database publicly available within **Suppl. Table 1**. An updateable version is also accessible within our R package (https://github.com/hagenaue/BrainInABlender) and as a downloadable spreadsheet (https://sites.google.com/a/umich.edu/megan-hastings-hagenauer/home/cell-type-analysis).

Citation	Subjects	Tissue	Purification Method	Platform	Stringency	Derived Cortical Cell Type Indices	Transcripts/ Orthologs
Cahoy et al., *J Neuro,* 2008.	Young transgenic mice	Forebrain	Fluorescent cell sorting using antibodies to deplete non-specific cell types	Affymetrix microarray	>20 Fold Enrichment	Astrocyte_All	73
						Neuron_All	80
						Oligodendrocyte_All	50
Zhang et al., *J Neuro* , 2014	Young transgenic mice	Cortex	Fluorescent cell sorting using antibodies to deplete non-specific cell types	RNA-Seq	Top 40 transcripts with >20 Fold Enrichment	Astrocyte_All	40
						Endothelial_All	40
						Microglia_All	40
						Mural_Pericyte	40
						Neuron_All	40
						Oligodendrocyte_Myelinating	40
						Oligodendrocyte_Newly-Formed	39
						Oligodendrocyte_Progenitor Cell	40
Zeisel et al., *Science,* 2015	Juvenile mice	Somatosensory cortex and CA1 hippocampus	Unbiased capture of single cells from whole tissue cell suspension	RNA-Seq	Enriched with 99.9% posterior probability	Astrocyte_All	240
						Endothelial_All	353
						Microglia_All	436
						Mural_All	155
						Neuron_Interneuron	365
						Neuron_Pyramidal_Cortical	294
						Oligodendrocyte_All	453
Darmanis et al., PNAS, 2015	Adult human epileptic patients	Anterior temporal lobe	Unbiased capture of single cells from whole tissue cell suspension	RNA-Seq	"Top 20" enriched transcripts	Astrocyte_All	21
						Endothelial_All	21
						Microglia_All	21
						Neuron_All	21
						Oligodendrocyte_Mature	21
						Oligodendrocyte_Progenitor Cell	21
Doyle et al., *Cell,* 2008	Young transgenic mice	Cortex, striatum, cerebellum, spinal cord, basal forebrain, and brain stem	Capture of translated mRNA from specific cell types labeled in transgenic mice using translating ribosome affinity purification (TRAP)	Affymetrix microarray	Top 25 enriched transcripts determined by iterative rank comparisons	Astrocyte_All	25
						Neuron_CorticoSpinal	25
						Neuron_CorticoStriatal	25
						Neuron_CorticoThalamic	25
						Neuron_Interneuron_CORT	25
						Neuron_Neuron_CCK	25
						Neuron_Neuron_PNOC	24
						Oligodendrocyte_All	25
						Oligodendrocyte_Mature	25
Daneman et al., *PLOS,* 2010	Young transgenic mice	Cortex	Fluorescent cell sorting using antibodies to deplete non-specific cell types	Affymetrix microarray	>20 Fold enrichment for endothelial, >8 fold enrichment for vasculature	Endothelial_All	49
						Mural_Vascular	50
Sugino et al., *Nature Neuro,* 2006	Transgenic mice	Cingulate and somatosensory cortices, basolateral amygdala, CA1-CA3 hippocampus, and dorsal LGN of the	Hand-sorting fluorescently-labeled cells followed by amplification	Affymetrix microarray	Enriched with p< 1.5E-11	Neuron_GABA	32
						Neuron_Glutamate	67
Gene card	Human	Human	Erythrocyte-related genes	Unknown	Unknown	RBC_All	17

Table 1. Thousands of transcripts have been identified as specifically-enriched in particular cortical cell types within published single-cell or purified cell type transcriptomic experiments. *The experimental and statistical methods for determining whether a transcript was enriched in a cell type varied by publication, and included both RNA-Seq and microarray datasets.*

92 **2.2 "*BrainInABlender*": Employing the Database of Cell Type Specific Transcripts to Predict**
93 **Relative Cell Type Balance in Heterogenous Brain Samples**

94 Next, we designed a method that uses the collective expression of cell type specific transcripts in
95 brain tissue samples to predict the relative cell type balance of the samples ("BrainInABlender"). We
96 specifically designed BrainInABlender to be compatible with large human brain transcriptional profiling
97 datasets such as those used by our research consortium (Pritzker) and the Allen Brain Institute, which
98 may lack full information about relative levels of expression within individual samples due to the
99 extensive normalization procedures used to combine data across batches or platforms. We have made our
100 method publicly-available in the form of a downloadable R package
101 (https://github.com/hagenaue/BrainInABlender).

102 In brief, BrainInABlender extracts the data from transcriptional profiling datasets that represent
103 genes identified in our database as having cell type specific expression in the brain (as curated by official
104 gene symbol). Prior to application of our method, the dataset should be in the format of expression-level
105 summary data (RNA-Seq: gene-level summary - CPM, RPKM or TPM; microarray: probe or probeset
106 summary), and should have received at least some basic preprocessing, including log(2) transformation,
107 normalization to eliminate technical variation, and standard quality control. Within BrainInABlender,
108 these data are then centered and scaled across samples (mean=0, sd=1) to prevent transcripts with more
109 variable signal from exerting disproportionate influence on the results. Then, if necessary, the normalized
110 data from all transcripts representing the same gene are averaged for each sample and re-scaled. Finally,
111 for each sample, these values are averaged across the genes identified as having expression specific to a
112 particular cell type for each reference publication included in the database of cell type specific transcripts.
113 This creates 38 cell type signatures derived from the cell type specific genes identified by the eight
114 publications ("Cell Type Indices"), each of which predicts the relative content for one of the 10 primary
115 cell types in our brain samples (**Figure 1**).

116 Later, during validation analyses (***Suppl. Section 7.2***), we found substantial support for simply
117 averaging these 38 publication-specific cell type indices within each of the primary categories to produce

ten consolidated primary cell-type indices for each sample. To perform this consolidation, we also removed any transcripts that were identified as "cell type specific" to multiple primary cell type categories (**Suppl. Figure 3**). These consolidated indices are included as output from BrainInABlender.

Please note that our method was specifically designed to tackle challenges present in our microarray data, but we later discovered that it bears some resemblance to the existing method of Population Specific Expression Analysis (PSEA, (10–12)). A more detailed discussion of the similarities and differences between the techniques can be found in ***Suppl. Section 7.2.2.***

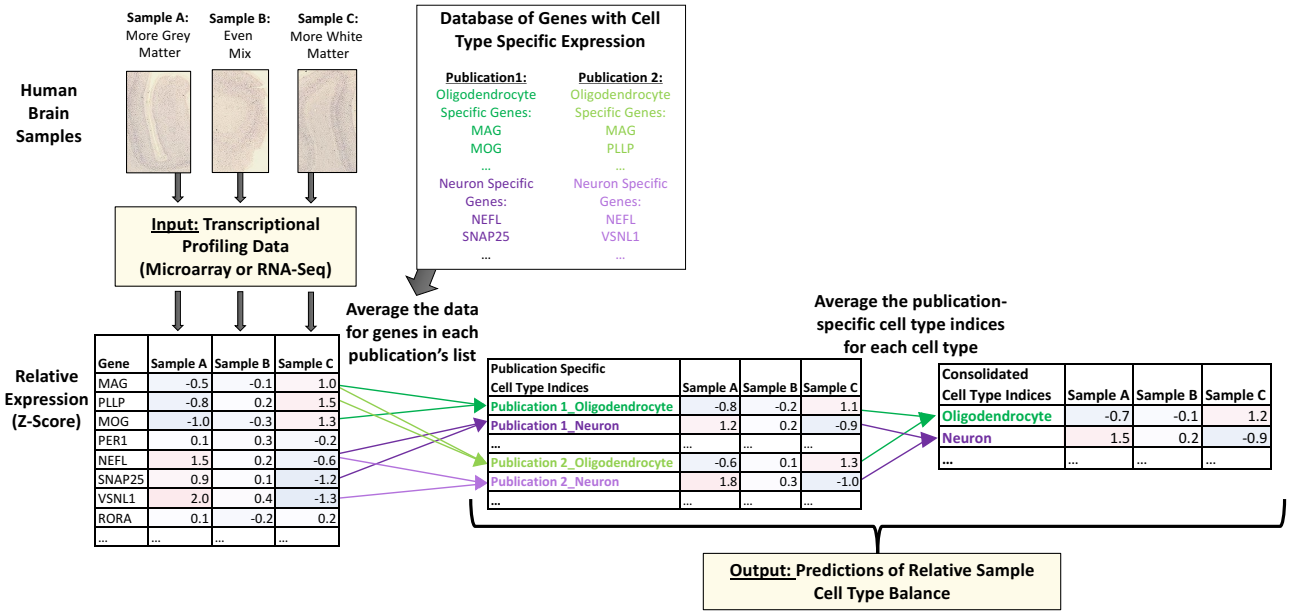

Figure 1. Predicting the relative cell type balance in human brain samples using genes previously-identified as having cell type specific expression. *Within macro-dissected brain tissue samples, variable cell type balance is likely to influence the pattern of gene expression. To estimate this variability, we extracted the data for genes that had been previously identified as having cell type specific expression in previous publications ("Database of genes with cell type specific expression", **Table 1**) and then averaged across the transcripts identified as specific to a particular cell type for each reference publication in our database to create 38 different "Cell Type Indices" that predicted relative cell content in each of the brain samples. Then, for many analyses in our paper, these publication-specific cell type indices were averaged within their cell type category to produce consolidated cell type indices representing each of the 10 primary cell types in the human cortex.*

137 **2.3 Validation of Relative Cell Content Predictions**

138 We initially validated our method using publicly-available datasets from purified cortical cell
139 types (RNA-seq datasets GSE52564 and GSE6783), artificial mixtures of cells produced *in silico* by
140 sampling from within these datasets, and microarray data from samples containing artificially-generated
141 mixtures of cultured cells from P1 pups (Affymetrix Rat Genome 230 2.0 Array dataset GSE19380;
142 further detail: ***Suppl. Sections 7.1.1- 7.1.2***). For each of these analyses, we examined the correlation
143 between the cell type indices outputted by BrainInABlender and the documented cell content of the
144 samples.

145 Next, we wanted to see whether the cell content predictions produced by BrainInABlender could
146 also correctly reflect relative cell type balance in human post-mortem samples. To test this, we applied
147 our method to a large human post-mortem Agilent microarray dataset (841 samples) spanning 160 cortical
148 and subcortical brain regions from the Allen Brain Atlas (http://human.brain-map.org/microarray/search,
149 December 2015, (25)). This dataset was derived from high-quality tissue (absence of neuropathology,
150 pH>6.7, post-mortem interval<31 hrs, RIN>5.5) from 6 human subjects (26). The tissue samples were
151 collected using a mixture of block dissection and laser capture microscopy (27). After applying
152 BrainInABlender, we compared the outputted cell type index results between selected brain regions
153 known to contain relatively more (+) or less (-) of a particular cell type using Welch's t-test (further
154 detail: ***Suppl. Section 7.1.4)***.

155

156 **2.4 Predicting Relative Cell Content in Transcriptomic Data from Macro-Dissected Human**
157 **Cortical Tissue from Psychiatric Subjects**

158 Next, we profiled cell type specific gene expression in several large psychiatric human brain
159 microarray datasets. The first was a large Pritzker Consortium Affymetrix U133A microarray dataset
160 derived from high-quality human post-mortem dorsolateral prefrontal cortex samples (final n=157
161 subjects), including tissue from subjects without a psychiatric or neurological diagnosis ("Controls",
162 n=71), or diagnosed with Major Depressive Disorder ("MDD", n=40), Bipolar Disorder ("BP", n=24), or

163 Schizophrenia ("Schiz", n= 22). The severity and duration of physiological stress at the time of death was
164 represented by an agonal factor score for each subject (ranging from 0-4, with 4 representing severe
165 physiological stress (28,29)). We measured the pH of cerebellar tissue to indicate the extent of oxygen
166 deprivation experienced around the time of death (28,29) and calculated the interval between the
167 estimated time of death and the freezing of the brain tissue (the postmortem interval or PMI) using
168 coroner records. Our current analyses began with subject-level summary gene expression data
169 (GSE92538).

170 We determined the replicability of our results using three smaller publicly-available post-mortem
171 human cortical Affymetrix U133Plus2 microarray datasets (GSE53987 (30), GSE21935 (31), GSE21138
172 (32), **Table 2.**). These datasets were selected because they included both psychiatric and control samples,
173 and provided pH, PMI, age, and gender in the demographic information on the GEO website
174 (https://www.ncbi.nlm.nih.gov/geo/). To control for technical variation, the sample processing batches
175 were estimated using the microarray chip scan dates extracted from the .CEL files and RNA degradation
176 was estimated using the R package AffyRNADegradation (33).

177 Finally, we also explored replicability within the recently-released large CommonMind
178 Consortium (CMC) human dorsolateral prefrontal cortex RNA-seq dataset (34); downloaded from the
179 CommonMind Consortium Knowledge Portal (https://www.synapse.org/CMC; final n=514 subjects). We
180 predicted the relative cell type content of these samples using a newer version of BrainInABlender (v2)
181 which excluded a few of the weaker cell type specific gene sets (15).

182 In general, the full preprocessing methods for these datasets can be found in ***Suppl. Section 7.1.***
183 The code for all analyses in the paper can be found at https://github.com/hagenaue/ and
184 https://github.com/aschulmann/CMC_celltype_index.

Microarray:

GEO Accession #	Published?	Brain Bank	Brain Region	Sample Size (no outliers)	Subjects per group (no outliers)	AVE pH (+/- SD)	AVE Age (+/- SD)	AVE PMI (+/- SD)	% Female
GSE92538	*Current paper:* Hagenauer (2018)	Pritzker Consortium: UC-Irvine	BA9/BA46	**337** (multiple replicates/ subject)	**157:** 71 CNTRL, 24 BP, 40 MDD, 22 SCHIZ	**6.8** (+/-0.3)	**52** (+/-15)	**24** (+/-9)	**27%**
GSE53987	Lanz et al. (2015)	PITT	BA46: *grey matter*	**66**	**66:** 18 CNTRL, 17 BP, 17 MDD, 14 SCHIZ	**6.6** (+/-0.3)	**46** (+/-10)	**20** (+/-6)	**45%**
GSE21935	Barnes et al. (2011)	CCHPC	BA22	**42**	**42:** 19 CNTRL, 23 SCHIZ	**6.3** (+/-0.3)	**70** (+/-19)	**8** (+/-5)	**45%**
GSE21138	Narayan et al. (2008)	MHRI	BA46: *grey matter*	**54**	**54:** 27 CNTRL, 27 SCHIZ	**6.3** (+/-0.2)	**45** (+/-17)	**40** (+/-13)	**17%**

RNA-Seq:

Public Data Release	Published?	Brain Bank	Brain Region	Sample Size (all)	Subjects per group (all)	AVE pH (+/- SD)	AVE Age (+/- SD)	AVE PMI (+/- SD)	% Female
Synapse.org	Fromer et al. (2016)	CommonMind Consortium: MSSM, PENN, PITT	BA9 / BA46 (PITT: *grey matter)*	**621**	**603:** 285 CNTRL, 263 SCZ, 47 BP, 8 AFF	**6.5** (+/- 0.3)	**65** (+/- 18) (binned 90+)	**17** +/- 11	**41%**

Table 2. We examined the pattern of cell-type specific gene expression in five post-mortem human cortical tissue datasets that included samples from subjects with psychiatric illness. *Abbreviations: CTRL: control, BP: Bipolar Disorder, MDD: Major Depressive Disorder, SCHIZ: Schizophrenia, GEO: Gene Expression Omnibus, BA: Brodmann's Area, PMI: Post-mortem interval, SD: Standard Deviation, Brain Banks: UC-Irvine (University of California – Irvine), PITT (University of Pittsburgh), CCHPC (Charing Cross Hospital Prospective Collection), MSSM (Mount Sinai Icahn School of Medicine), MHRI (Mental Health Research Institute Australia), PENN (University of Pennsylvania)*

3.5 Examining the Relationship Between Predicted Cell Content Derived from Transcriptional Profiling Data and Clinical/Biological Variables

We next set out to observe the relationship between the predicted cell content of our samples and a variety of medically-relevant subject variables. To perform this analysis, we first examined the relationship between seven relevant subject variables and each of the ten consolidated cell type indices in the Pritzker prefrontal cortex dataset using a linear regression model that allowed us to simultaneously control for other likely confounding variables:

Equation 1:

$$\text{Cell Type Index} = \beta 0 + \beta 1*(\text{Brain pH}) + \beta 2*(\text{Agonal Factor}) + \beta 3*(\text{PMI}) + \beta 4*(\text{Age}) + \beta 5*(\text{Sex}) + \beta 6*(\text{Diagnosis}) + \beta 7*(\text{Exsanguination}) + \varepsilon$$

We then examined the replicability of these relationships using data from the three smaller publicly-available human post-mortem microarray datasets (GSE53987, GSE21935, GSE21138). For these datasets, we initially lacked detailed information about manner of death (agonal factor and exsanguination), but were able to control for technical variation within the model using statistical estimates of RNA degradation and batch (scan date):

Equation 2:

$$\text{Cell Type Index} = \beta 0 + \beta 1*(\text{Brain pH}) + \beta 2*(\text{PMI}) + \beta 3*(\text{Age}) + \beta 4*(\text{Sex}) + \beta 5*(\text{Diagnosis}) + \beta 6*(\text{RNA Degradation}) + \beta 7*(\text{Batch, } \textit{when applicable}) + \varepsilon$$

We evaluated replicability by performing a meta-analysis for each variable and cell type combination across the four microarray datasets. To do this, we applied random effects modeling to the respective betas and accompanying sampling variance derived from each dataset using the *rma.mv()* function within the *metafor* package (35). P-values were corrected for multiple comparisons following the Benjamini-Hochberg method (FDR or q-value; (36)).

Finally, we characterized these relationships in the large CMC RNA-seq dataset. For this dataset, we had some information about manner of death but lacked knowledge of agonal factor or exsanguination. We controlled for technical variation due to dissection site (institution) and RNA degradation (RIN):

Equation 3:

$$\text{Cell Type Index} = \beta 0 + \beta 1*(\text{Brain pH}) + \beta 2*(\text{PMI}) + \beta 3*(\text{Age}) + \beta 4*(\text{Sex}) + \beta 5*(\text{Diagnosis}) + \beta 6*(\text{RNA Degradation}) + \beta 7*(\text{Institution}) + \beta 8*(\text{MannerOfDeath}) + \varepsilon$$

3.6 Characterizing Psychiatric Gene Expression using Differential Expression Models that Include Either Standard Co-variates or Cell Type Indices

To determine whether controlling for variability in cell type balance in the dataset could improve our ability to detect differential expression related to psychiatric illness, we compared differential expression results within the human psychiatric datasets that were derived from linear regression models of increasing complexity, including a simple base model containing just the variable of interest ("Model 1"), a standard model controlling for traditional co-variates ("Model 2"), and a model controlling for

traditional co-variates as well as each of the cell type indices ("Model 5"). We also used two reduced models that only included the most prevalent cell types (Astrocyte, Microglia, Oligodendrocyte, Neuron_Interneuron, Neuron_Projection; (21)) to avoid issues with multicollinearity. The first of these models included traditional co-variates ("Model 4"), whereas the second model excluded them ("Model 3") (**Equation 4**).

Equation 4: A model of gene expression for each dataset, colored to illustrate the subcomponents evaluated during our model comparison (#M1-M5). *The base model (intercept and variable of interest) is presented in green, traditional subject variable covariates are blue, the cell type indices for the most prevalent cell types are red, and the remaining cell type indices are purple. Model components unique to each dataset are underlined.*

The Pritzker microarray dataset:
Gene Expression (Probeset Signal) =
β0 + β1*(The variable of interest: Diagnosis)
+β2*(Brain pH)+ β3*(PMI)+ β4*(Age)+ β5*(Sex)+ β6*(Agonal Factor)+
+ β7*(Astrocyte)+β8*(Oligodendrocyte)+β9*(Microglia)+β10*(Interneuron)+β11*(ProjectionNeuron)
+β12*(Endothelial)+β13*(Neuron_All)+β14*(Oligodendrocyte_Immature)+β15*(Mural)+β16*(RBC)+ ε

The CMC RNA-Seq dataset:
Gene Expression (Probeset Signal) =
β0 + β1*(The variable of interest: Diagnosis)
+β2*(Brain pH)+β3*(PMI)+ β4*(Age)+ β5*(Sex)+ β6*(RIN)+β7*(Institution)+ β8*(CauseOfDeath)+
+ β9*(Astrocyte)+β10*(Oligodendrocyte)+β11*(Microglia)+β12*(Interneuron)+β13*(ProjectionNeuron)
+β14*(Endothelial)+β15*(Neuron_All)+β16*(Oligodendrocyte_Immature)+β17*(Mural)+β18*(RBC)+ ε

The smaller microarray datasets (GSE53987, GSE21935, GSE21138):
Gene Expression (Probeset Signal) =
β0 + β1*(The variable of interest: Diagnosis)
+β2*(Brain pH)+β3*(PMI)+ β4*(Age)+ β5*(Sex)+ β6*(RNADegradation)+
+ β7*(Astrocyte)+β8*(Oligodendrocyte)+β9*(Microglia)+β10*(Interneuron)+β11*(ProjectionNeuron)
+β12*(Endothelial)+β13*(Neuron_All)+β14*(Oligodendrocyte_Immature)+β15*(Mural)+β16*(RBC)+ ε

3.7 Functional Ontology with Cell Type Specific Gene Sets

We ran a series of analyses to evaluate how well we could distinguish between changes in cell type balance in the tissue and changes in cell type specific functions. First, as a case study, we specifically examined the relationship between age and the functional annotation for genes found in the Neuron_All index in more depth. To do this, we evaluated the relationship between age and gene expression in the Pritzker dataset using a standard model that controlled for traditional confounds ("Model 2") using the

signal data for all probesets in the dataset. We used "DAVID: Functional Annotation Tool" (//david.ncifcrf.gov/summary.jsp, (37,38) to identify the functional clusters that were overrepresented by the genes included in our neuronal cell type index (using the full HT-U133A chip as background), and then determined the average effect of age (beta) for the genes included in each of the 240 functional clusters. These functional clusters overrepresented dendritic/axonal related functions, so for a follow-up analysis, in a manner that was blind to the results, we subsetted the results into 29 functional clusters that were clearly related to dendritic/axonal functions and 41 functional clusters that seemed distinctly unrelated to dendritic/axonal functions (**Suppl. Table 4**) and compared the average effect of age in these two subsets using a Welch's t-test.

In the next analysis, we decided to make the process of differentiating between altered cell type-specific functions and relative cell type balance more efficient. We used our cell type specific gene lists to construct gene sets in a file format (.gmt) compatible with the popular tool Gene Set Enrichment Analysis (GSEA, (39,40)) and combined them with two other commonly-used gene set collections from the molecular signatures database (MSigDB: http://software.broadinstitute.org/gsea/msigdb/index.jsp, downloaded 09/2017, "C2: Curated Gene Sets" and "C5: GO Gene Sets", **Suppl. Table 5**). Then we tested the utility of incorporating our new gene sets into GSEA (fGSEA: (41)) using the ranked results (betas) for the relationship between each subject variable and each probeset in the Pritzker dataset (as evaluated using a standard model: "Model 2").

3. Results & Discussion

3.1 Validation of Relative Cell Content Predictions

Validation Using Datasets Derived from Purified or Cultured Cells: We initially validated our method using publicly-available datasets from purified cell types (datasets GSE52564 and GSE6783; (2,18) and *in silico* derived mixtures and found that the statistical cell type indices easily predicted the cell

type identities of the samples (***Suppl. Section 7.2.10***). Therefore, as further validation, we determined whether relative cell type balance could be accurately deciphered from microarray data for samples containing artificially-generated mixtures of cultured cells (GSE19380; (12)). We found that the consolidated cell type indices produced by BrainInABlender strongly correlated with the actual percentage of cells of a particular type included in the artificial mixtures (**Figure 2**, Neuron% vs. Neuron_All Index: R^2=0.93, p=1.54e-15, Astrocyte% vs. Astrocyte Index: R^2=0.77, p=5.05e-09, Microglia% vs. Microglia Index: R^2=0.64, p=8.2e-07), although we found that the cell type index for immature oligodendrocytes better predicted the percentage of cultured oligodendrocytes in the samples than the cell type index for mature oligodendrocytes (Mature: R^2=0.45, p=0.000179, Immature: R^2=0.81, p=4.14e-10). We believe this discrepancy is likely to reflect the specific cell culture conditions used in the original admixture experiment. Notably, the relationship between the consolidated cell type indices and the actual percentage of each cell type included in the artificial mixtures was approximately linear, despite the use of log(2)-transformed expression data.

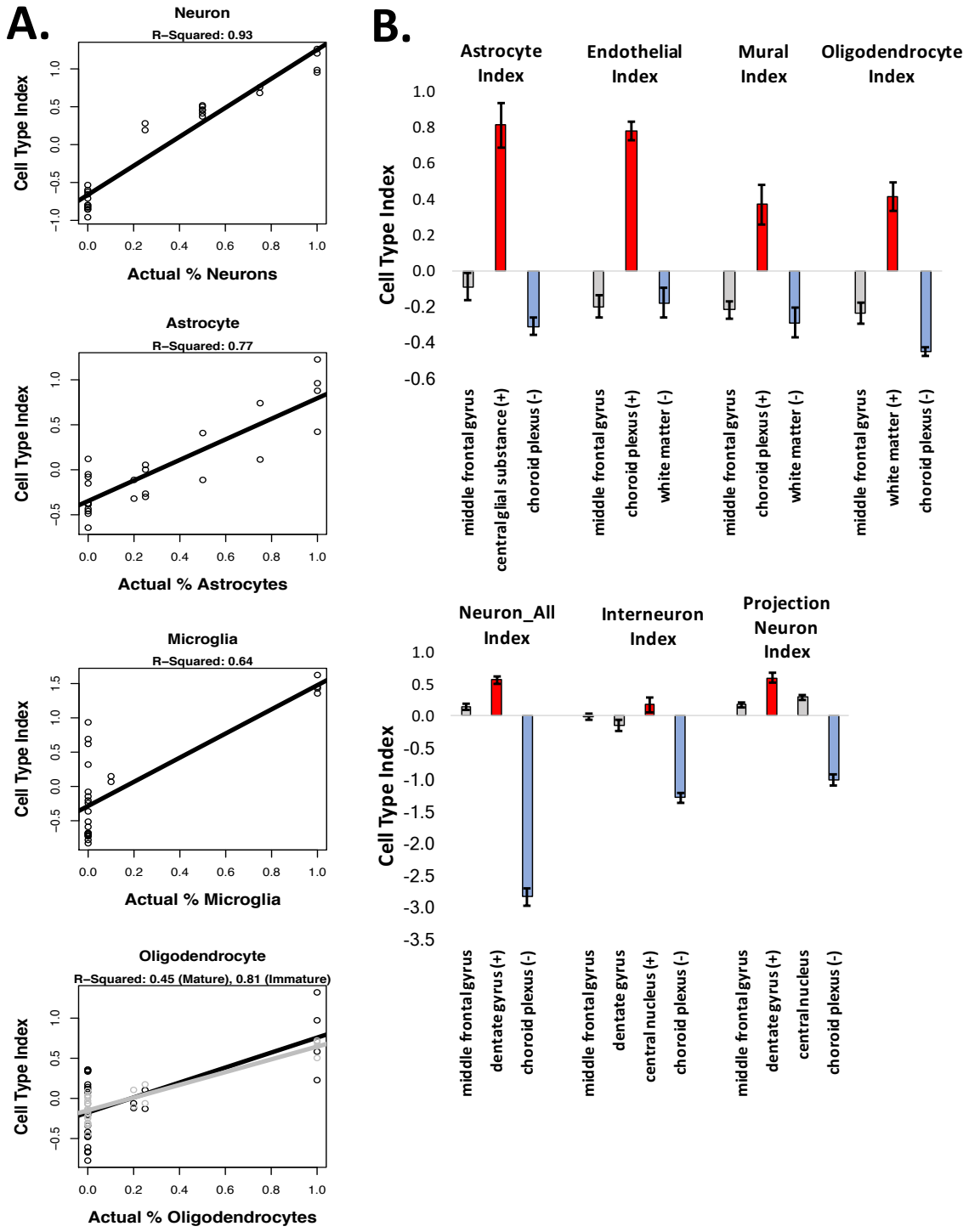

Figure 2. Validation of Relative Cell Content Predictions. *A) Using a microarray dataset derived from samples that contained artificially-generated mixtures of cultured cells (GSE19380; (12)), we found that our relative cell content predictions ("cell type indices") closely reflected actual known content. However, note that the numeric values for the cell type indices do not convey an absolute proportion of cells of a particular type in the sample - simply whether a sample contains relatively more or less of the cell type of interest in comparison to other samples in the dataset. B) Our cell type indices also easily*

differentiated human post-mortem samples derived from brain regions that are known to contain relatively more (+, red) or less (-, blue) of the targeted cell type of interest (all p<0.007). Results from the middle frontal gyrus are included for comparison, since the rest of the paper primarily focuses on prefrontal cortical data. (Bars: average +/-SE).

Validation Using a Dataset Derived from Human Post-Mortem Tissue: Next, we wanted to see whether the cell content predictions produced by BrainInABlender correctly reflected relative cell type balance in human post-mortem samples. To test this, we applied our method to a large cross-regional human post-mortem microarray dataset (25), and extracted the results for a selection of brain regions that are known to contain relatively more (+) or less (-) of particular cell types (the results for other regions can be found in **Suppl. Table 2**). The results clearly indicated that our cell type analyses could identify well-established differences in cell type balance across brain regions (**Figure 2,** (+) region vs. (-) region for all cell types: $p<0.007$, Cohen's $d>3.2$). The choroid plexus had elevated gene expression specific to vasculature (endothelial cells, mural cells, (42)). The corpus callosum and cingulum bundle showed an enrichment of oligodendrocyte-specific gene expression (42). The central glial substance was enriched with gene expression specific to glia and support cells, especially astrocytes. The dentate gyrus, which contains densely-packed glutamatergic granule cells (43), was enriched for gene expression specific to projection neurons. The highly GABA-ergic central nucleus of the amygdala (44) had a slight enrichment of gene expression specific to interneurons. These results provide fundamental validation that our methodology can accurately predict relative cell type balance in human post-mortem samples. Moreover, these results suggest that the cell type indices are capable of generally tracking their respective cell types in subcortical structures, despite the dependency of our method on cell type specific gene lists derived from the forebrain and cortex.

335 **3.8 Inferred Cell Type Composition Explains a Large Percentage of the Sample-Sample Variability**
336 **in Transcriptomic Data from Macro-Dissected Human Cortical Tissue**

337 Using principal components analysis we found that the primary gradients of gene expression
338 variation across samples in all four of the cortical transcriptomic datasets strongly correlated with our
339 estimates of cell type balance. For example, while analyzing the Pritzker microarray dataset, we found
340 that the first principal component (PC1), which encompassed 23% of the variation in gene expression
341 across samples in the dataset, spanned from samples with high predicted support cell content to samples
342 with high predicted neuronal content. Therefore, a large percentage of the variation in PC1 (91%) was
343 accounted for by an average of the astrocyte and endothelial indices (p=2.2e-82, with a respective R^2 of
344 0.80 and 0.75 for each index analyzed separately) or by the general neuron index (p=6.3e-32, R^2=0.59).
345 The second notable gradient in the dataset (PC2) encompassed 12% of the variation overall, and spanned
346 samples with high predicted projection neuron content to samples with high predicted oligodendrocyte
347 content (with a respective R^2 of 0.62 and 0.42, and p-values of p=8.5e-35 and p=8.7e-20).

348 To confirm that the strong relationship between the top principal components of variation and our
349 cell type indices did not originate artificially due to cell type specific genes representing a large
350 percentage of the most highly variable transcripts in the dataset, we repeated the principal components
351 analysis after excluding all cell type specific transcripts from the dataset and still found these strong
352 correlations (**Figure 3;** PC1 vs. average astrocyte/endothelial index: R^2=0.89, p=1.1e-76; PC2 vs.
353 projection neuron index: R^2=0.65, p=1.6e-37). Indeed, individual cell type indices still better accounted
354 for the main principal components of variation in the microarray data than *all other major subject*
355 *variables combined* (pH, Agonal Factor, PMI, Age, Gender, Diagnosis; PC1: R^2=0.416, PC2: R^2=0.203).
356 Similarly, when examining the data for individual probesets, a linear model that included just the six
357 subject variables (**Equation 4**) accounted for an average of only 12% of the variation (R^2,
358 Adj.R^2=0.0692), whereas a linear model including the astrocyte and projection neuron indices alone
359 accounted for 17% (R^2, Adj.R^2=0.156) and a linear model including all 10 cell types accounted for an
360 average of 30% (R^2, Adj.R^2=0.255), almost one third of the variation present in the data for any particular

361 probeset. Therefore, a large percentage of the genes in our dataset seemed to be preferentially expressed
362 in relationship to particular cell types, even if their expression was not defined as strictly cell type specific
363 in our database.

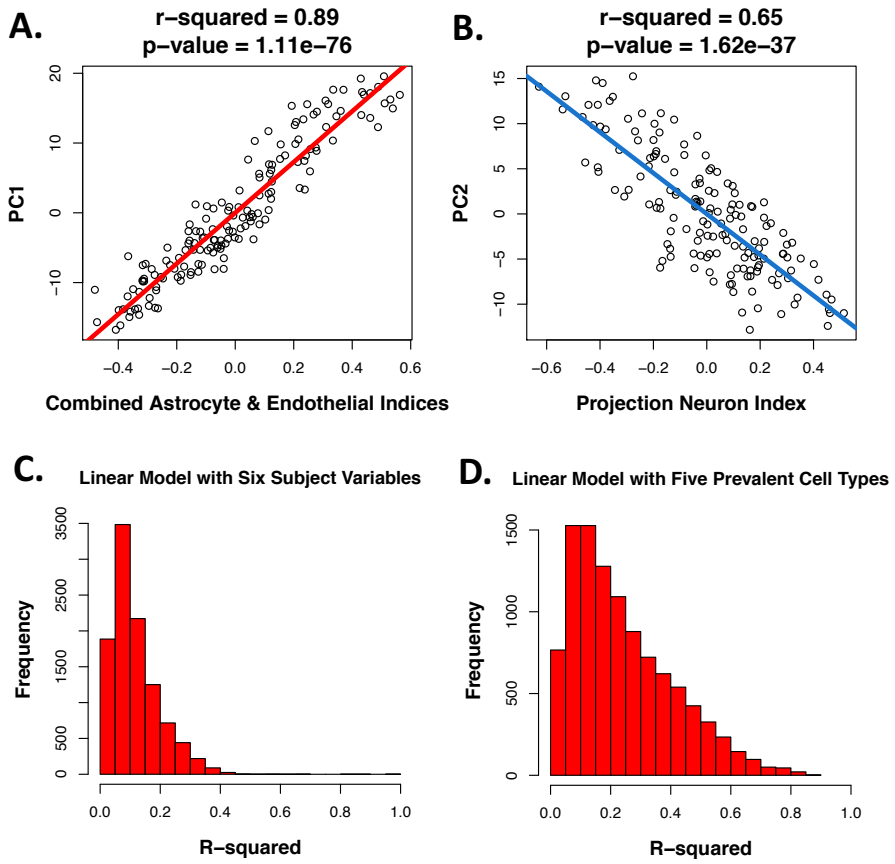

364

365 ***Figure 3. Cell content predictions explain a large percentage of the variability in microarray data***
366 ***derived from the human cortex.*** *As an example, within the Pritzker dataset, even after excluding all data*
367 *from genes identified as cell type specific in our database,* ***A)*** *the first principal component of variation*
368 *(PC1) was strongly correlated with predicted "support cell" content in the samples (the average of the*
369 *astrocyte and endothelial indices).* ***B)*** *PC2 was strongly correlated with predicted projection neuron*
370 *content. Likewise, when applying a linear model to the data for each probeset, the* R^2 *values for each*
371 *probeset (illustrated in the histogram) tended to be much smaller when using a model that included* ***C)***
372 *only the six subject variables, versus* ***D)*** *only the five most prevelant cortical cell types.*

373

374 Within the other four human cortical tissue datasets, the relationships between the top principal
375 components of variation and the consolidated cell type indices were similarly strong (***Suppl. Section 3.8***),
376 despite the fact that these datasets had received less preprocessing to remove the effects of technical
377 variation. These results indicated that accounting for cell type balance is important for the interpretation

378 of post-mortem human brain transcriptomic data and might improve the signal-to-noise ratio in analyses
379 aimed at identifying psychiatric risk genes.

380 **3.9 Cell Content Predictions Derived from Transcriptional Profiling Data Match Known**
381 **Relationships Between Clinical/Biological Variables and Brain Tissue Cell Content**

382 We next set out to observe the relationship between the predicted cell content of our samples and a
383 variety of medically-relevant subject variables. This analysis uncovered many relationships that had been
384 previously-identified using other paradigms or animal models (**Figure 4, Suppl. Table 3**).

385 ***Dissection:*** First, as a proof of principle, we were able to clearly observe dissection differences
386 between institutions within the large CMC RNA-Seq dataset, with samples from University of Pittsburgh
387 having a predicted relative cell type balance that closely matched what would be expected due to their
388 gray matter only dissection method (Oligodendrocyte: β =-0.404, p=2.42e-11; Microglia: β=-0.274,
389 p=3.06e-05; Neuron_Interneuron: β=0.0916, p=0.0161; Neuron_Projection: β=0.145, p=2.31e-05; Mural:
390 β=0.170, p=2.14e-08; Endothelial: β=0.200, p=1.12e-05). In contrast, samples from University of
391 Pennsylvania were associated with lower predicted cell content related to vasculature (Endothelial: β=-
392 0.255, p=4.01-04; Mural: β=-0.168, p=4.59e-04; Astrocyte: β=-0.189, p=7.47e-03).

393 ***Manner of Death:*** Predicted cell type content was also closely related to manner of death. Within the
394 Pritzker dataset we found that subjects who died in a manner that involved exsanguination had a notably
395 low red blood cell index (β=-0.398; p=0.00056). Later, we were able replicate this result within
396 GSE21138 using data from 5 subjects who were also likely to have died in a manner involving
397 exsanguination (β=-0.516, p=0.052**trend,* manner of death reported in suppl. in *(32)*).

398 The presence of prolonged hypoxia around the time of death, as indicated by either low brain pH or
399 high agonal factor score within the Pritzker dataset, was associated with a large increase in the endothelial
400 cell index (Agonal Factor: β=0.118 p=2.85e-07; Brain pH: β=-0.210, p=0.0003) and astrocyte index
401 (Brain pH: β=-0.437, p=2.26e-07; Agonal Factor: β=0.071, p=0.024), matching previous demonstrations
402 of cerebral angiogenesis, endothelial and astrocyte activation and proliferation in low oxygen

403 environments (45). Smaller increases were also seen in the mural index (Mural vs. Agonal Factor: β=
404 0.0493, p=0.0286). In contrast, prolonged hypoxia was associated with a clear decrease in all of the
405 neuronal indices (Neuron_All vs. Agonal Factor: β=-0.242, p=3.58e-09; Neuron_All vs. Brain pH:
406 β=0.334, p=0.000982; Neuron_Interneuron vs. Agonal Factor: β=-0.078, p=4.13e-05;
407 Neuron_Interneuron vs. Brain pH: β=0.102, p=0.034; Neuron_Projection vs. Agonal Factor: β=-0.096, p=
408 0.000188), mirroring the notorious vulnerability of neurons to low oxygen (e.g., (46)).
409 These overall effects of hypoxia on predicted cell type balance replicated in the smaller human
410 microarray post-mortem datasets (Astrocyte vs. Brain pH (meta-analysis: b=-0.459, p=2.59e-11):
411 GSE21138: β=-0.856, p=0.00661, GSE53987: β=-0.461, p=0.00812, Neuron_All vs. Brain pH (meta-
412 analysis: b= 0.245, p=7.72e-04), Neuron_Interneuron vs. Brain pH (meta-analysis: b=0.109, p=7.89e-03):
413 GSE21138: β=0.381134, p=0.0277), despite lack of information about agonal factor, and partially
414 replicated in the CMC human RNA-Seq dataset (Neuron_Interneuron vs. Brain pH: β=0.186, p=9.81e-
415 05). In several datasets, we also found that prolonged hypoxia correlated with a decreased microglial
416 index (Microglia vs. Brain pH: GSE53987: β=0.462, p=0.00603; CMC: β=0.286, p=4.66e-04).
417

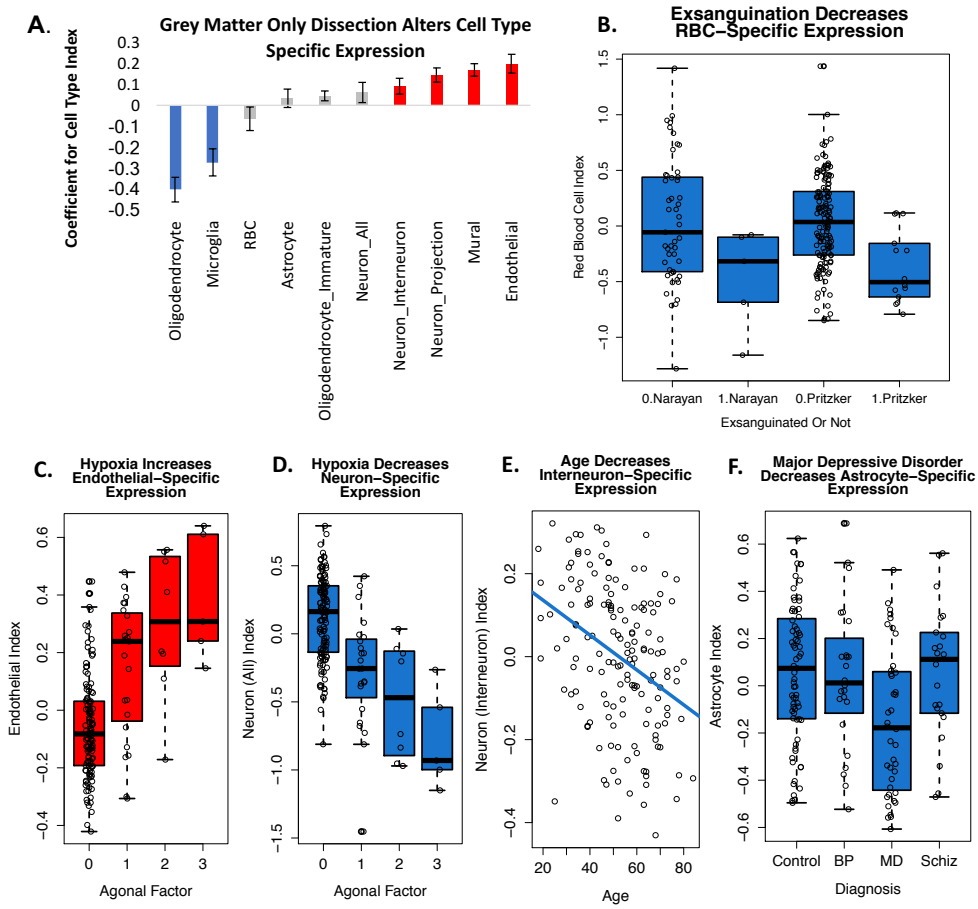

G. The most highly replicated effects across datasets:

	Pritzker	Lanz et al. 2015	Barnes et al. 2011	Narayan et al. 2008	Meta-Analysis: Nominal P-value	Meta-Analysis: FDR (q-value)	CMC	CMC: Nominal P-value	CMC: FDR (q-value)	Replication in Microarray Meta-analysis and CMCC
Hypoxia:										
Astrocyte vs. Brain pH	**-5.4**	**-2.7**	-1.1	**-2.9**	2.59E-11	2.33E-09	**2.1**	3.25E-02	9.55E-02	
Neuron_All vs. Brain pH	**3.4**	0.1	1.3	1.9	7.72E-04	1.16E-02	0.6	5.60E-01	7.00E-01	*
Neuron_Interneuron vs. Brain pH	**2.1**	1.0	-0.5	**2.3**	7.89E-03	5.52E-02	**3.9**	9.81E-05	6.69E-04	**
Microglia vs. Brain pH	-1.0	**2.9**	-0.1	1.9	5.41E-01	7.91E-01	**3.5**	4.66E-04	2.59E-03	*
Oligodendrocyte_Immature vs. Brain pH	**-3.0**	0.4	-0.5	1.4	1.40E-01	3.71E-01	**3.0**	2.68E-03	1.22E-02	
Age										
Neuron_All vs. Age	-1.9	**-2.1**	-1.2	-1.2	1.57E-03	2.02E-02	**-4.3**	2.27E-05	1.93E-04	**
Neuron_Interneuron vs. Age	**-3.4**	-0.5	**-2.5**	**-2.5**	2.91E-06	6.56E-05	**-6.5**	2.10E-10	3.15E-09	**
Neuron_Projection vs. Age	**-2.8**	**-3.7**	-0.5	**-3.1**	1.61E-06	4.83E-05	**-7.5**	2.93E-13	7.33E-12	**
Oligodendrocyte vs. Age	1.8	1.2	0.3	**3.1**	2.74E-03	2.74E-02	1.6	1.02E-01	2.25E-01	*
Oligodendrocyte_Immature vs. Age	**-3.7**	**-4.7**	-0.2	**-4.5**	5.98E-11	2.69E-09	**-11.0**	3.32E-25	2.49E-23	**
PMI										
Oligodendrocyte vs. PMI	**-3.6**	**-3.6**	-1.6	-0.5	2.23E-05	4.02E-04	**-4.1**	4.70E-05	3.36E-04	**
Endothelial vs. PMI	-2.0	-0.8	0.4	-0.1	5.51E-02	2.36E-01	**-3.9**	1.32E-04	8.60E-04	*
Microglia vs. PMI	-1.0	-1.5	-1.2	-0.7	9.72E-02	3.05E-01	**-3.5**	5.15E-04	2.76E-03	*
Oligodendrocyte_Immature vs. PMI	**3.5**	1.0	1.6	-0.4	4.81E-03	4.33E-02	-0.4	6.86E-01	8.04E-01	
Neuron_Projection vs. PMI	**3.9**	1.6	-0.2	-1.2	2.28E-03	2.56E-02	**3.1**	1.97E-03	9.24E-03	**
Neuron_All vs. PMI	**2.5**	1.8	-0.4	0.0	1.74E-02	9.81E-02	**2.6**	1.10E-02	3.88E-02	*
Diagnosis:										
Astrocyte vs. Diagnosis_MDD	**-2.6**	-1.0			5.88E-03	4.81E-02				
Neuron_All vs. Diagnosis BP	-0.9	-0.7			2.46E-01	5.39E-01	**2.6**	8.44E-03	3.17E-02	
RBC vs. Diagnosis_Schiz	-1.2	0.1	-1.0	-0.5	2.04E-01	4.96E-01	**-2.5**	1.41E-02	4.71E-02	*
Gender:										
Neuron_Interneuron vs. GenderFemale	-0.9	0.0	0.7	0.3	6.65E-01	9.06E-01	**-2.5**	1.20E-02	4.09E-02	
Neuron_Projection vs. GenderFemale	1.0	-0.3	-0.4	1.6	3.60E-01	6.46E-01	**-2.5**	1.11E-02	3.88E-02	

419 ***Figure 4. Cell content predictions derived from microarray data match known relationships between***
420 ***subject variables and brain tissue cell content.*** *Boxplots represent the median and interquartile range,*
421 *with whiskers illustrating either the full range of the data or 1.5x the interquartile range.* ***A.*** *Within the*
422 *CMC dataset, cortical tissue samples that were dissected to only contain gray matter (PITT) show lower*
423 *predicted oligodendrocyte and microglia content and more neurons and vasculature (bars: β+/- SE,*
424 *red/blue: p<0.05).* ***B.*** *Subjects who died in a manner that involved exsanguination had a notably low red*
425 *blood cell index in both the Pritzker (p=0.00056) and Narayan et al. datasets (p=0.052**trend). ***C.*** *The*
426 *presence of prolonged hypoxia around the time of death, as indicated by high agonal factor score, was*
427 *associated with a large increase in the endothelial cell index (p=2.85e-07) matching previous*
428 *demonstrations of cerebral angiogenesis, activation, and proliferation in low oxygen environments (45).*
429 ***D.*** *High agonal factor was also associated with a clear decrease in neuronal indices (p=3.58e-09)*
430 *mirroring the vulnerability of neurons to low oxygen (46).* ***E.*** *Age was associated with a decrease in the*
431 *neuronal indices (p= 0.000956) which fits known decreases in gray matter density in the frontal cortex in*
432 *aging humans (47).* ***F****. Major Depressive Disorder was associated with a moderate decrease in astrocyte*
433 *index (p= 0.0118), which fits what has been observed morphometrically (48).* ***G.*** *The most highly-*
434 *replicated relationships between subject variables and predicted cortical cell content across all five of the*
435 *post-mortem human datasets. Provided in the table are the T-stats for the effects (red=upregulation,*
436 *blue=downregulation), derived from a larger linear model controlling for confounds* ***(Equation 1,***
437 ***Equation 2, Equation 3****), as well as the nominal p-values from the meta-analysis of the results across the*
438 *four microarray studies, and p-values following multiple-comparisons correction (q-value). Only effects*
439 *that had a q<0.05 in either our meta-analysis or the large CMC RNA-Seq dataset are included in the*
440 *table. Asterisks denote effects that had consistent directionality in the meta-analysis and CMC dataset (*)*
441 *or consistent directionality and q<0.05 in both datasets (**). Please note that lower pH and higher*
442 *agonal factor are both indicators of greater hypoxia prior to death, but have an inverted relationship and*
443 *therefore show opposing relationships with the cell type indices.*

444

445 ***Age:*** In the Pritzker dataset, age was associated with a moderate decrease in two of the neuronal
446 indices (Neuron_Interneuron vs. Age: β=-0.00291, p=0.000956; Neuron_Projection Neuron vs. Age: β=-
447 0.00336, p=0.00505) and this was strongly replicated in the large CMC RNA-Seq dataset (Neuron_All vs.
448 Age: β=-0.00497, p=2.27e-05; Neuron_Projection Neuron vs. Age: β=-0.00612, p=2.93e-13;
449 Neuron_Interneuron vs. Age: β=-0.00591, p=2.10e-10). A similar decrease in predicted neuronal content
450 was seen in all three of the smaller human post-mortem datasets (Neuron_All vs. Age (meta-analysis: b=-
451 0.00415, p=1.57e-03): GSE53987: β=-0.00722, p=0.0432, Neuron_Interneuron vs. Age (meta-analysis:
452 b=-0.00335, p=2.91e-06): GSE21138: β=-0.00494, p=0.0173, GSE21935: β=-0.00506, p=0.0172,
453 Neuron_Projection vs. Age (meta-analysis: b=-0.00449, p=1.61e-06): GSE53987: β=-0.0103,
454 p=0.000497, GSE21138: β=-0.00763, p=0.00386). This result mirrors known decreases in gray matter
455 density in the frontal cortex in aging humans (47), as well as age-related sub-region specific decreases in
456 frontal neuron numbers in primates (49) and rats (50).

There was a consistent decrease in the immature oligodendrocyte index in relationship to age across datasets (Oligodendrocyte_Immature vs. Age (meta-analysis: b=-0.00514, p=5.98e-11): Pritzker: β=-0.00432, p=0.000354, GSE21138: β=-0.00721, p=5.73e-05, GSE53987: β=-0.00913, p=1.85e-05; CMC: β=-0.00621, p=3.32e-25), which seems intuitive, but actually contradicts animal studies on the topic (51). Since the validation of the immature oligodendrocyte index was relatively weak (***Suppl. Section 7.2***), this result should perhaps be considered with caution.

In some datasets, there also appeared to be an increase in the oligodendrocyte index with age (Oligodendrocyte vs. Age (meta-analysis: b=0.00343, p=2.74e-03): GSE21138, β=0.00957, p=0.00349) which, at initial face value, seems to contrast with well-replicated observations that frontal white matter decreases with age in human imaging studies (47,52,53). However, it is worth noting that several histological studies in aging primates suggest that brain regions that are experiencing demyelination with age actually show an *increasing* number of oligodendrocytes due to repair (51,54).

PMI: A prominent unexpected effect was a large decrease in the oligodendrocyte index with longer post-mortem interval (Oligodendrocyte vs. PMI (meta-analysis: b=-0.00764, p=2.23e-05): Pritzker: β=-0.00749, p=0.000474, GSE53987: β=-0.0318, p=0.000749; CMC: β=-0.00759, p=4.70e-05). Upon further investigation, we found a publication documenting a 52% decrease in the fractional anisotropy of white matter with 24 hrs post-mortem interval as detected by neuroimaging (55), but to our knowledge the topic is otherwise not well studied. These changes were paralleled by a decrease in the endothelial index (CMC: β=-0.00542, p=1.32e-04) and microglial index (CMC: β=-0.00710, p=5.15e-04) and increase in the immature oligodendrocyte index (Oligodendrocyte_Immature vs. PMI (meta-analysis: b=0.00353, p=4.81e-03): Pritzker: β=0.00635, p=0.000683) and neuronal indices (Neuron_All vs. PMI: Pritzker: β=0.006997, p=0.000982; CMC: β=0.00386, p=0.0110; Neuron_Projection vs. PMI (meta-analysis: b=0.00456, p=2.28e-03): Pritzker: β= 0.00708, p=1.64e-04; CMC: β=0.00331, p=0.00197). These results could arise from the zero-sum nature of transcriptomics analysis: due to the use of a standardized dissection size, RNA concentration, and data normalization, if there are large decreases in gene

482 expression for one common variety of cell type (oligodendrocytes), then gene expression related to other
483 cell types may appear to increase.

484 ***Psychiatric Diagnosis:*** Of most interest to us were potential changes in cell type balance in relation
485 to psychiatric illness. In previous post-mortem morphometric studies, there was evidence of glial loss in
486 the prefrontal cortex of subjects with Major Depressive Disorder, Bipolar Disorder, and Schizophrenia
487 (reviewed in (56)). This decrease in glia, and particularly astrocytes, was replicated experimentally in
488 animals exposed to chronic stress (57), and when induced pharmacologically, drove animals into a
489 depressive-like condition (57). Replicating the results of (48), we observed a moderate decrease in
490 astrocyte index in the prefrontal cortex of subjects with Major Depressive Disorder (meta-analysis:
491 b=0.132, p=5.88e-03, Pritzker: β =-0.133, p=0.0118, **Figure 4 F**), but did not see similar changes in the
492 brains of subjects with Bipolar Disorder or Schizophrenia.We also observed a decrease in red blood cell
493 index in association with Schizophrenia (CMC: β=-0.104, p=0.0141) which is tempting to ascribe to
494 reduced blood flow due to hypofrontality (58). This decrease in red blood cell content could also arise due
495 to psychiatric subjects having an increased probability of dying a violent death, but the effect remained
496 present when we controlled for exsanguination, and therefore is likely to be genuinely tied to the illness
497 itself.

498 ***General Discussion:*** Overall, these results indicate that statistical predictions of the cell content of
499 samples effectively capture many known biological changes in cell type balance, and imply that within
500 both chronic (age, diagnosis) and acute conditions (agonal, PMI, pH) there is substantial influences upon
501 the relative representation of different cell types.

502 The effect of hypoxia within our results is particularly worth discussing in greater depth. It has been
503 acknowledged for a long time that exposure to a hypoxic environment prior to death has a huge impact on
504 gene expression in human post-mortem brains (e.g., (28,29,59–61)). This impact on gene expression is so
505 large that up until recently the primary principal component of variation (PC1) in our data was assumed to
506 represent the degree of hypoxia, and was sometimes even removed before performing diagnosis-related
507 analyses (e.g., (62)). These large effects of hypoxia on gene expression were hypothesized to be partially

508 mediated by neuronal necrosis (63) and lactic acidosis (60). However, the magnitude of the effect of
509 hypoxia was still puzzling, especially when compared to the much more moderate effects of post-mortem
510 interval (even when ranging from 8-40+ hrs). Our current analysis provides an explanation for this
511 discrepancy, since it is clear from our results that the brains of our subjects are *actively compensating* for
512 a hypoxic environment prior to death by altering the balance or overall transcriptional activity of support
513 cells and neurons. The differential effects of hypoxia on neurons and glial cells have been studied since
514 the 1960's (64), but to our knowledge this is the first time that anyone has related the large effects of
515 hypoxia in post-mortem transcriptomic data to a corresponding upregulation in the transcriptional activity
516 of vascular cell types (45).

517 This connection is important for understanding why results associating gene expression and
518 psychiatric illness in human post-mortem tissue sometimes do not replicate. If a study contains mostly
519 tissue from individuals who experienced greater hypoxia before death (e.g., hospital care with artificial
520 respiration or coma), then differential expression analyses are likely to inadvertently focus on
521 neuropsychiatric effects in support cell types, whereas a study that mostly contains tissue from individuals
522 who died a fast death (e.g., myocardial infarction) will emphasize the neuropsychiatric effects in neurons.
523 That said, although both indicators of perimortem hypoxia (agonal factor and pH) showed similar strong
524 relationships with cell type balance, we recommend caution when interpreting the relationship between
525 pH and cell type in tissue from psychiatric subjects, as pH can indicate other biological changes besides
526 hypoxia. For example, there are small consistent decreases in pH associated with Bipolar Disorder even in
527 live subjects (65–67) and metabolic changes associated with pH are theorized to play an important role in
528 Schizophrenia (61). Therefore, the relationship between pH and cell type balance may be partially driven
529 by a third variable (psychiatric illness or treatment). It is also possible that changes in tissue cell content
530 could cause a change in pH (68).
531

532 **3.10 It is Difficult to Discriminate Between Changes in Cell Type Balance and Cell-Type Specific**
533 **Function**

534 Gray matter density has been shown to decrease in the frontal cortex in aging humans (47), and
535 frontal neuron numbers decrease in specific subregions in aging primates (49) and rats (50). However,
536 many scientists would argue that age-related decreases in gray matter are primarily driven by synaptic
537 atrophy instead of decreased cell number (69). This raised the question of whether the decline that we saw
538 in neuronal cell indices with age was being largely driven by the enrichment of genes related to synaptic
539 function in the index. More generally, it raised the question of how well cell type indices could
540 discriminate changes in cell number from changes in cell-type function.

541 We examined this question using two methods. First, as a case study, we specifically examined the
542 relationship between age and the functional annotation for genes found in the Neuron_All index in more
543 depth. We found that transcripts from functional clusters that seemed distinctly unrelated to
544 dendritic/axonal functions still showed an average decrease in expression with age (T(40)=-2.7566,
545 p=0.008756), but this decrease was larger for transcripts clearly associated with dendritic/axonal-related
546 functions (T(28)=-4.5612, p=9.197e-05; dendritic/axonal vs. non-dendritic/axonal: T(50.082)=2.3385,
547 p=0.02339, **Suppl. Figure 11**). Based on this analysis, we conclude that synaptic atrophy could be
548 partially driving age-related effects on neuronal cell type indices in the human prefrontal cortex dataset
549 but are unlikely to fully explain the relationship.

550 Next, we decided to make the process of differentiating between altered cell type-specific functions
551 and relative cell type balance more efficient. We used our cell type specific gene lists to construct gene
552 sets in a file format (.gmt) compatible with the popular tool Gene Set Enrichment Analysis (39,40). Then,
553 for the results from each subject variable within the Pritzker dataset, we compared the enrichment of the
554 effects within gene sets defined by brain cell type to the enrichment seen within gene sets for other
555 functional categories. In general, we found that gene sets for brain cell types tended to be the top result
556 (most extreme normalized enrichment score, NES) for each of the subject variables that showed a strong
557 relationship with cell type in our previous analyses (Agonal Factor vs.

558 "Neuron_All_Cahoy_JNeuro_2008": NES=-2.46, p=0.00098, q=0.012, Brain pH vs.
559 "Astrocyte_All_Cahoy_JNeuro_2008": NES=-2.48, p=0.0011, q=0.014, MDD vs.
560 "Astrocyte_All_Cahoy_JNeuro_2008": NES=-2.60, p=0.0010, q=0.017, PMI vs.
561 "GO_OLIGODENDROCYTE_DIFFERENTIATION": NES=-2.42, p=0.00078, q=0.027; **Suppl. Table**
562 **6**). Similarly, the relationship between the effects of age and neuron-specific gene expression was ranked
563 #4, following the gene sets "GO_SYNAPTIC_SIGNALING",
564 "REACTOME_TRANSMISSION_ACROSS_CHEMICAL_SYNAPSES",
565 "REACTOME_OPIOID_SIGNALLING", but each of them was assigned a similar p-value (p=0.001) and
566 adjusted p-value (q=0.036). We conclude that it is important to consider cell type-specific expression
567 during the analysis of macro-dissected brain microarray data above and beyond the consideration of
568 specific functional pathways, and have submitted our .gmt files to the Broad Institute for addition to their
569 curated gene sets in MSigDB to promote this form of analysis.
570

571 **3.11 Including Cell Content Predictions in the Analysis of Microarray Data Improves Model Fit**
572 **and Enhances the Detection of Diagnosis-Related Genes in Some Datasets**

573 Over the years, many researchers have been concerned that transcriptomic analyses of
574 neuropsychiatric illness often produce non-replicable or contradictory results and, perhaps more
575 disturbingly, are typically unable to replicate well-documented effects detected by other methods. We
576 posited that this lack of sensitivity and replicability might be partially due to cell type variability in the
577 samples, especially since such a large percentage of the principal components of variation in our samples
578 were explained by neuron to glia ratio. Within the Pritzker dataset, we were particularly interested in
579 controlling for cell type variability, because dissection may have differed between technical batches that
580 were unevenly distributed across diagnosis categories (**Figure 5 A**). There was a similarly uneven
581 distribution of dissection methods across diagnosis categories within the large CMC RNA-Seq dataset. In
582 this dataset, the majority of the bipolar samples (75%) were collected by a brain bank that performed gray

583 matter only dissections (PITT), whereas the control and schizophrenia samples were more evenly
584 distributed across all three institutions (34).

585 We hypothesized that controlling for cell type while performing differential expression analyses
586 in these datasets would improve our ability to detect previously-documented psychiatric effects on gene
587 expression, especially psychiatric effects that were previously-identified within specific cell types, since
588 these effects should not be mediated by psychiatric changes in overall cell type balance. To test the
589 hypothesis, we first compiled a list of 130 strong, previously-documented relationships between
590 Schizophrenia or Psychosis and gene expression in particular cell types in the human cortex, as detected
591 by *in situ* hybridization or immunocytochemistry ((70–75) reviewed further in (19)) or by single-cell type
592 laser capture microscopy (**Suppl. Figure 12, Suppl. Table 7** (1,76,77)).

593 As a comparison, we also considered lists of transcripts strongly-associated with Schizophrenia
594 (78) and Bipolar Disorder (79) in meta-analyses of microarray data derived from human frontal cortical
595 tissue (**Suppl. Figure 12**, **Suppl. Table 7**). The effects of psychiatric illness on the expression of these
596 transcripts could be mediated by either psychiatric effects on cell type balance or by effects within
597 individual cells. Therefore, controlling for cell type balance while performing differential expression
598 analyses could detract from the detection of some psychiatric effects, but perhaps also enhance the
599 detection of other psychiatric effects by controlling for large, confounding sources of noise (*e.g.,*
600 dissection variability).

601 Next, we examined our ability to detect these previously-documented psychiatric effects using
602 regression models of increasing complexity (**Figure 5 B**), including a standard model controlling for
603 traditional co-variates (Model 2) and models controlling for cell type co-variates (Models 3-5).

A. Diagnosis Effects May Be Partially Confounded By Dissection Variability

Pritzker:	
Samples	**Batch***
Control	All Batches
BP, MDD	1-4, 9-13
Schiz	5-8, 13-15

**Batches partially defined by subject cohort*

CMC:	
Samples	**Institution***
Controls	All (PITT, MSSM, PENN)
BP	PITT, MSSM
Schiz	All (PITT, MSSM, PENN)

**PITT was a grey matter only dissection*

B.

	Model Complexity
M1	***Base Model:*** Diagnosis Only
M2	***Standard Model:*** Diagnosis + Traditional Co-variates
M3	Diagnosis + Most Prevalent Cell Types
M4	Diagnosis + Traditional Co-variates + Most Prevalent Cell Types
M5	Diagnosis + Traditional Co-variates + All Cell Types

C. All Expressed Genes: Model Fit Improves After Adding Cell Type

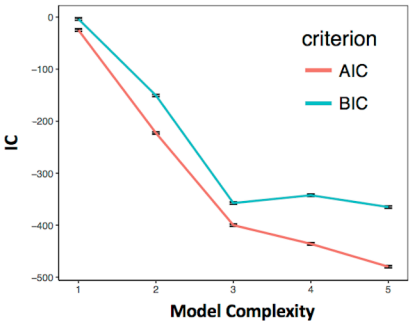

D. Genes with Previously-Identified Psychiatric Effects: Model Fit Improves After Adding Cell Type

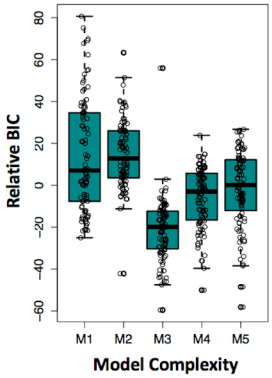

E. Controlling for Cell Type Variability Enhances Detection of Psychiatric Effects in Some Datasets

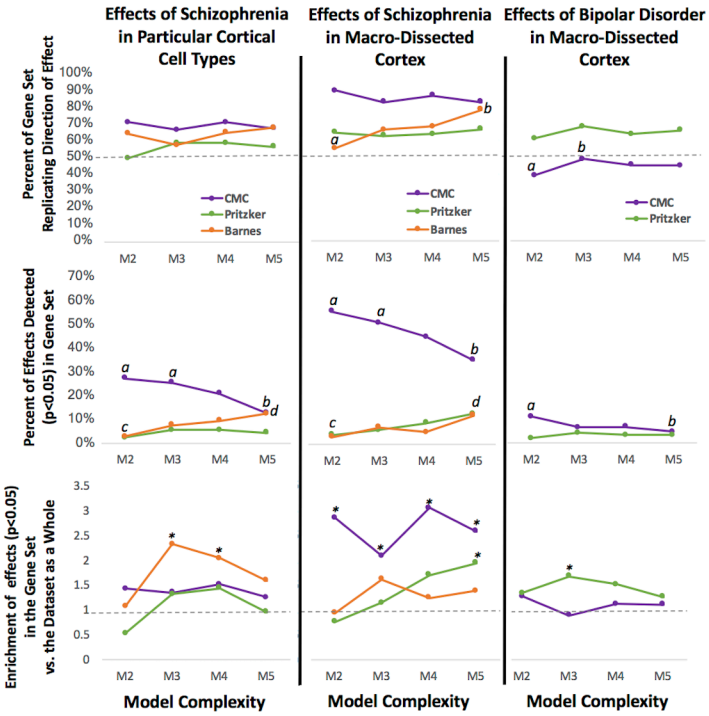

604

Figure 5. Including Cell Content Predictions in the Analysis of Microarray Data Improves Model Fit and Enhances the Detection of Previously-Identified Diagnosis-Related Genes in Some Datasets. A. *Diagnosis effects were likely to be partially confounded by dissection variability within the Pritzker and CMC datasets.* ***B:*** *We examined a series of differential expression models of increasing complexity, including a base model (M1), a standard model (M2), and three models that included cell type co-variates (M3-M5).* ***C-D.*** *Model fit improved with the addition of cell type (M1/M2 vs. M3-M5) when examining either* ***C****. all expressed genes in the dataset (example from CMC: points= AVE +/-SE).* ***D.*** *genes with previously-documented relationships with psychiatric illness in particular cell types (example from Pritzker: BIC values for all models for each gene were centered prior to analysis. Boxes represent the median and interquartile range of the data).* ***E.*** *Evaluating the replication of previously-observed psychiatric effects (**Suppl. Figure 12**) in three datasets (Pritzker, CMC, and Barnes) using a standard differential expression model (M2) vs. models that include cell type co-variates (M3-5). Letters (a vs. b, c vs. d) denote significant model comparisons (Fisher's exact test: p<0.05). Top graphs: The percentage of genes (y-axis: 0-1) replicating the direction of previously-documented psychiatric effects on cortical gene expression sometimes increases with the addition of cell type to the model (p<0.05: Barnes (effects of Schiz): M2 vs. M5, CMC (effects of Bipolar Disorder): M2 vs. M3). Middle graphs: The detection of previously-identified psychiatric effects on gene expression (p<0.05 & replicated direction of effect) increases with the addition of cell type to the model in some datasets (p<0.05, Barnes: M2 vs. M5, Pritzker: M2 vs. M5) but decreases in others (p<0.05, CMC: M2 vs. M5, M3 vs. M5). Bottom graphs: In some datasets we see an enrichment of psychiatric effects (*p<0.05) in previously-identified psychiatric gene sets only after controlling for cell type (Barnes: M3, M4, Pritzker: M5, M3). For the CMC dataset, we see an enrichment using all models (*p<0.05).*

We found that including predictions of cell type balance in our models assessing the effect of diagnosis on gene expression dramatically improved model fit as assessed by Akaike's Information Criterion (AIC) or Bayesian Information Criterion (BIC). These improvements were largest with the addition of the five most prevalent cell types to the model (M3, M4); the addition of less common cell types produced smaller gains (M5). These improvements were clear whether we considered the average model fit for all expressed genes (*e.g.,* **Figure 5 C**) or just genes with previously-identified psychiatric effects (*e.g.,* **Figure 5 D**).

However, models that included cell type were not necessarily superior at replicating previously-observed psychiatric effects on gene expression, even when examining psychiatric effects that were likely to be independent of changes in cell type balance. For each model, we quantified the percentage of genes replicating the previously-observed direction of effect in relationship to psychiatric illness, as well as the percentage of genes that replicated the effect using a common threshold for detection (p<0.05). Finally, we also looked at the enrichment of psychiatric effects (p<0.05) in each of the previously-documented

641 psychiatric gene sets in comparison to the other genes in our datasets (genes universally represented in all
642 three datasets- Pritzker, CMC, Barnes).

643 In general, we found that the two datasets that had the most variability in gene expression related
644 to cell type (Pritzker, Barnes) were more likely to replicate previously-documented psychiatric effects on
645 gene expression when the differential expression model included cell type covariates. For example, in the
646 Barnes dataset, adding cell type co-variates to the model increased our ability to detect effects of
647 Schizophrenia that had been previously documented within particular cell types or macro-dissected tissue
648 (**Figure 5E**, Fisher's exact test: M2 vs. M5, $p<0.05$ in both gene sets) and revealed an enrichment of
649 Schizophrenia effects in genes with previously-documented psychiatric effects in particular cell types
650 (Fisher's exact test $p<0.05$: M3 & M4). In the Pritzker dataset, adding cell type co-variates to the model
651 increased our ability to detect previously-documented effects of Schizophrenia in macrodissected tissue
652 (M2 vs. M5: $p<0.05$) and revealed a significant enrichment of Schizophrenia and Bipolar effects in genes
653 with previously-documented psychiatric effects in macro-dissected tissue (Fisher's exact test $p<0.05$:
654 Schizophrenia: M5, Bipolar: M3). This mirrored the results of another analysis that we had conducted
655 suggesting that controlling for cell type increased the overlap between the top diagnosis results in the
656 Pritzker dataset and previous findings in the literature as a whole (***Suppl. Section 7.3.4***).

657 In the large CMC RNA-Seq dataset, the rate of replication of previously-documented effects of
658 Schizophrenia was already quite high using a standard differential expression model containing traditional
659 co-variates (M2). Using a standard model, we could detect 27% of the previously-documented effects in
660 cortical cell types and 55% of the previously-documented effects in macro-dissected tissue (with a
661 replicated direction of effect and $p<0.05$). However, in contrast to what we had observed in the Pritzker
662 and Barnes datasets, controlling for cell type *diminished* the ability to detect effects of Schizophrenia that
663 had been previously-observed within particular cell types or macrodissected tissue in a manner that scaled
664 with the number of co-variates included in the model (M2 or M3 vs. M5: $p<0.05$ for both gene sets),
665 despite improvements in model fit parameters and a lack of significant relationship between
666 Schizophrenia and any of the prevalent cell types. Including cell type co-variates in the model did not

667 improve our ability to observe an enrichment of Schizophrenia effects in genes with previously-
668 documented psychiatric effects in macro-dissected tissue (all models showed enrichment, M2-M5:
669 Fisher's exact test $p<0.05$). Controlling for cell type slightly improved the replication of the direction of
670 previously-documented Bipolar Disorder effects (Fisher's exact test: M2 vs. M3: $p<0.05$) in a manner that
671 would seem appropriate due to the highly uneven distribution of bipolar samples across institutions and
672 dissection methods, but even after this improvement the rate of replication was still no better than chance
673 (48%), and, counterintuitively, the ability to successfully detect those effects still diminished in a manner
674 that seemed to scale with the number of co-variates included in the model (Fisher's exact test: M2 vs. M5,
675 $p<0.05$). In a preliminary analysis of the two smaller human microarray datasets that were derived from
676 gray-matter only dissections (GSE53987, GSE21138), the addition of cell type co-variates to differential
677 expression models clearly diminished both the percentage of genes replicating the previously-documented
678 direction of effect of Schizophrenia in particular cell types (Fisher's exact test: GSE21138: M2 vs. M4 or
679 M5: $p<0.05$, GSE53987: M2 vs. M4 or M5: $p<0.05$) and the ability to successfully detect previously-
680 documented effects (Fisher's exact test: GSE21138: M2 vs. M4 or M5: $p<0.05$).

681 ***General Discussion***: We found that including cell type indices as co-variates while running
682 differential expression analyses helped improve our ability to detect previously-documented relationships
683 between psychiatric illness and gene expression in human cortical datasets that were particularly affected
684 by variability in cell type balance. This improvement was not seen in datasets that were less affected by
685 variability in cell type balance, despite improvements in model fit and a lack of strong multicollinearity
686 between diagnosis and the cell type indices. This finding was initially surprising to us, but upon further
687 consideration makes sense, as the cell type indices are multi-parameter gene expression variables.
688 Therefore, there is increased risk of overfitting when modeling the data for any particular gene. We
689 conclude that the addition of cell type covariates to differential expression models is only recommended
690 when there is a particularly large amount of variability in the dataset associated with cell type balance, or
691 when there is strong reason to believe that technical variation associated with cell type (such as
692 dissection) may be highly confounding in the result. We strongly recommend that model selection while

693 conducting differential expression analyses should be considered carefully, and evaluated not only in
694 terms of fit parameters but also validity and interpretability.

695 Regarding the importance of model selection for interpretability, it is worth noting that an
696 important difference between our final analysis methods and those used by some previous researchers
697 (*e.g.,* 10–12) was the lack of cell type interaction terms included in our models (*e.g.,* Diagnosis*Astrocyte
698 Index). Theoretically, the addition of cell type interaction terms should allow the researcher to statistically
699 interrogate cell-type differentiated diagnosis effects because samples that contain more of a particular cell
700 type should exhibit more of that cell type's respective diagnosis effect. Versions of this form of analysis
701 have been successful in other investigations (e.g., (11,12,80)) but we were not able to validate the method
702 using a variety of model specifications and our database of previously-documented relationships with
703 diagnosis in prefrontal cell types. Upon consideration, we realized that these negative results were
704 difficult to interpret because significant diagnosis*cell type interactions should only become evident if the
705 effect of diagnosis in a particular cell type is different from what is occurring in all cell types on average.
706 For genes with expression that is reasonably specific to a particular cell type (*e.g.,* GAD1, PVALB), the
707 overall average diagnosis effect may already largely reflect the effect within that cell type and the
708 respective interaction term will not be significantly different, even though the disease effect is clearly
709 tracking the balance of that cell population. In the end, we decided that the addition of interaction terms to
710 our models was not demonstrably worth the associated decrease in overall model fit and statistical power.
711 For public use we have released the full differential expression results for each dataset analyzed using the
712 different models discussed above **(Suppl. Table 8-Suppl. Table 12).**

713 **4. Conclusion and Future Directions**

714 In this manuscript, we have demonstrated that the statistical cell type index is a relatively simple
715 manner of interrogating cell-type specific expression in transcriptomic datasets from macro-dissected
716 human brain tissue. We find that statistical estimations of cell type balance almost fully account for the
717 top principal components of variation in microarray data derived from macro-dissected brain tissue

718 samples, far surpassing the effects of traditional subject variables (post-mortem interval, hypoxia, age,
719 gender). Indeed, our results suggest that many variables of medical interest are themselves accompanied
720 by strong changes in cell type specific gene expression in naturally-observed human brains. We find that
721 within both chronic (age, sex, diagnosis) and acute conditions (agonal, PMI, pH) there may be substantial
722 changes in the relative representation of different cell types. Thus, accounting for demography at the
723 cellular population level can be as important for the interpretation of microarray data as cell-level
724 functional regulation. This form of data deconvolution was useful for identifying the subtler effects of
725 psychiatric illness within our samples, divulging the decrease in astrocytes that is known to occur in
726 Major Depressive Disorder and the decrease in red blood cell content in the frontal cortex in
727 Schizophrenia, resembling known fMRI hypofrontality. This form of data deconvolution may also aid in
728 the detection of psychiatric effects while conducting differential expression analyses in datasets that have
729 highly-variable cell content.

730 These results touch upon the fundamental question as to whether organ-level function responds to
731 challenge by changing the biological states of individual cells or the life and death of different cell
732 populations. To reach such a sweeping perspective in human brain tissue using classic cell biology
733 methods would require epic efforts in labeling, cell sorting, and counting. We have demonstrated that
734 scientists can approximate this vantage point using an elegant, supervised signal decomposition exploiting
735 increasingly available genomic data. However, it should be noted that, similar to other forms of functional
736 annotation, cell type indices are best treated as a hypothesis-generation tool instead of a final conclusion
737 regarding tissue cell content. We have demonstrated the utility of cell type indices for detecting large-
738 scale alterations in cell content in relationship with known subject variables in post-mortem tissue. We
739 have not tested the sensitivity of the technique for detecting smaller effects or the validity under all
740 circumstances or non-cortical tissue types. Likewise, while using this technique it is impossible to
741 distinguish between alterations in cell type balance and cell-type specific transcriptional activity: when a
742 sample shows a higher value of a particular cell type index, it could have a larger number of such cells, or
743 each cell could have produced more of its unique group of transcripts, via a larger cell body, slower

744 mRNA degradation, or an overall change in transcription rate. In this regard, the index that we calculate
745 does not have a specific interpretation; rather it is a holistic property of the cell populations, the "neuron-
746 ness" or "microglia-ness" of the sample. Such an abstract index represents the ecological shifts inferred
747 from the pooled transcriptome. That said, our cell type indices do have real biological meaning - they can
748 be interpreted in a known system of cell type taxonomy. When single-cell genomic data uncovers new
749 cell types (e.g., the Allen Brain Atlas cellular taxonomy initiative (81)) or meta-analyses refine the list of
750 genes defined that have cell-type specific expression (e.g., (82)), our indices will surely evolve with these
751 new classification frameworks, but the power of the approach will remain, in that we can disentangle the
752 intrinsic changes of individual genes from the population-level shifts of major cell types.

753 Our work drives home the fact that any comprehensive theory of psychiatric illness needs to
754 account for the dichotomy between the health of individual cells and that of their ecosystem. We found
755 that the functional changes accompanying psychiatric illness in the cortex occurred both at the level of
756 cell population shifts (decreased astrocytic presence and red blood cell count) and at the level of intrinsic
757 gene regulation not explained by population shifts. A similar conclusion regarding the importance of cell
758 type balance in association with psychiatric illness was recently drawn by our collaborators (e.g.,(83))
759 using a similar technique to analyze RNA-Seq data from the anterior cingulate cortex. In the future, we
760 plan to use our technique to re-analyze many other large transcriptomic datasets with the hope of gaining
761 better insight into psychiatric disease. This application of our technique seems particularly important in
762 light of recent evidence linking disrupted neuroimmunity (84) and neuroglia (e.g., (48,57,85)) to
763 psychiatric illness, as well as growing evidence that growth factors with cell type specific effects play an
764 important role in depressive illness and emotional regulation (for a review see (23,86)).

765 In conclusion, we have found this method to be a valuable addition to traditional functional
766 ontology tools as a manner of improving the interpretation of transcriptomic results. For the benefit of
767 other researchers, we have made our database of brain cell type specific genes (**Suppl. Table 1**,
768 https://sites.google.com/a/umich.edu/megan-hastings-hagenauer/home/cell-type-analysis) and code for
769 conducting cell type analyses publicly available in the form of a downloadable R package

770 (https://github.com/hagenaue/BrainInABlender) and we are happy to assist researchers in their usage for
771 pursuing better insight into psychiatric illness and neurological disease.
772

773 **5. Acknowledgements**

774 We thank all members of the Pritzker Consortium (especially the University of California, Irvine
775 Brain Bank staff), Drs. Adriana Medina and David Krolewski for brain dissections and methodological
776 input, and Dr. Simon Evans, Sharon Burke and Mary Hoverstein for their involvement in the initial
777 mRNA extraction and microarrays. Grace Hsienyuan Chang, Jennifer Fitzpatrick, LeAnn Fitzpatrick, Jim
778 Stewart, Tom Dixon, Doug Smith, Andy Lin, and Manhong Dai were invaluable for maintaining our
779 databases of clinical information and biological specimens. Drs. Elyse Aurbach, Katherine Prater,
780 Kathryn Hilde, Fan Meng, Lilah Toker, Mark Reimers, and Angela O'Connor provided insightful advice
781 and feedback regarding the methodology or manuscript. Our undergraduate research assistants Isabelle
782 Birt, Alek Pankonin, and Daniela Romero Vargas helped compile the Allen Brain Atlas data, annotate and
783 upload code, create the BrainInABlender R package, and provide editorial assistance. Finally, we would
784 like to thank our reviewers, whose insightful feedback helped inspire several particularly useful analyses,
785 leading us to a stronger set of conclusions.

6. References

1. Arion D, Corradi JP, Tang S, Datta D, Boothe F, He A, et al. Distinctive transcriptome alterations of prefrontal pyramidal neurons in schizophrenia and schizoaffective disorder. Mol Psychiatry. 2015 Nov;20(11):1397–405.

2. Darmanis S, Sloan SA, Zhang Y, Enge M, Caneda C, Shuer LM, et al. A survey of human brain transcriptome diversity at the single cell level. Proc Natl Acad Sci U S A. 2015 Jun 9;112(23):7285–90.

3. Lake BB, Ai R, Kaeser GE, Salathia NS, Yung YC, Liu R, et al. Neuronal subtypes and diversity revealed by single-nucleus RNA sequencing of the human brain. Science. 2016 Jun 24;352(6293):1586–90.

4. Choi KH, Elashoff M, Higgs BW, Song J, Kim S, Sabunciyan S, et al. Putative psychosis genes in the prefrontal cortex: combined analysis of gene expression microarrays. BMC Psychiatry. 2008;8:87.

5. Evans SJ, Choudary PV, Neal CR, Li JZ, Vawter MP, Tomita H, et al. Dysregulation of the fibroblast growth factor system in major depression. Proc Natl Acad Sci U S A. 2004 Oct 26;101(43):15506–11.

6. Abbas AR, Wolslegel K, Seshasayee D, Modrusan Z, Clark HF. Deconvolution of blood microarray data identifies cellular activation patterns in systemic lupus erythematosus. PloS One. 2009;4(7):e6098.

7. Chikina M, Zaslavsky E, Sealfon SC. CellCODE: a robust latent variable approach to differential expression analysis for heterogeneous cell populations. Bioinforma Oxf Engl. 2015 May 15;31(10):1584–91.

8. Gaujoux R, Seoighe C. CellMix: a comprehensive toolbox for gene expression deconvolution. Bioinforma Oxf Engl. 2013 Sep 1;29(17):2211–2.

9. Shen-Orr SS, Gaujoux R. Computational deconvolution: extracting cell type-specific information from heterogeneous samples. Curr Opin Immunol. 2013 Oct;25(5):571–8.

10. Capurro A, Bodea L-G, Schaefer P, Luthi-Carter R, Perreau VM. Computational deconvolution of genome wide expression data from Parkinson's and Huntington's disease brain tissues using population-specific expression analysis. Front Neurosci. 2014;8:441.

11. Kuhn A, Kumar A, Beilina A, Dillman A, Cookson MR, Singleton AB. Cell population-specific expression analysis of human cerebellum. BMC Genomics. 2012;13:610.

12. Kuhn A, Thu D, Waldvogel HJ, Faull RLM, Luthi-Carter R. Population-specific expression analysis (PSEA) reveals molecular changes in diseased brain. Nat Methods. 2011 Nov;8(11):945–7.

13. Cahoy JD, Emery B, Kaushal A, Foo LC, Zamanian JL, Christopherson KS, et al. A transcriptome database for astrocytes, neurons, and oligodendrocytes: a new resource for understanding brain development and function. J Neurosci Off J Soc Neurosci. 2008 Jan 2;28(1):264–78.

822 14. Daneman R, Zhou L, Agalliu D, Cahoy JD, Kaushal A, Barres BA. The mouse blood-brain barrier
823 transcriptome: a new resource for understanding the development and function of brain endothelial
824 cells. PloS One. 2010;5(10):e13741.

825 15. Doyle JP, Dougherty JD, Heiman M, Schmidt EF, Stevens TR, Ma G, et al. Application of a
826 translational profiling approach for the comparative analysis of CNS cell types. Cell. 2008 Nov
827 14;135(4):749–62.

828 16. Sugino K, Hempel CM, Miller MN, Hattox AM, Shapiro P, Wu C, et al. Molecular taxonomy of
829 major neuronal classes in the adult mouse forebrain. Nat Neurosci. 2006 Jan;9(1):99–107.

830 17. Zeisel A, Muñoz-Manchado AB, Codeluppi S, Lönnerberg P, La Manno G, Juréus A, et al. Brain
831 structure. Cell types in the mouse cortex and hippocampus revealed by single-cell RNA-seq.
832 Science. 2015 Mar 6;347(6226):1138–42.

833 18. Zhang Y, Chen K, Sloan SA, Bennett ML, Scholze AR, O'Keeffe S, et al. An RNA-sequencing
834 transcriptome and splicing database of glia, neurons, and vascular cells of the cerebral cortex. J
835 Neurosci Off J Soc Neurosci. 2014 Sep 3;34(36):11929–47.

836 19. Lewis DA, Sweet RA. Schizophrenia from a neural circuitry perspective: advancing toward rational
837 pharmacological therapies. J Clin Invest. 2009 Apr;119(4):706–16.

838 20. Lynch JC. The Cerebral Cortex. In: Fundamental Neuroscience. 2nd ed. Philadelphia: Churchill
839 Livingstone; 2002. p. 505–20.

840 21. Hutchins DE, Naftel JP, Ard MD. The cell biology of neurons and glia. In: Fundamental
841 Neuroscience. 2nd ed. Philadelphia: Churchill Livingstone; 2002. p. 15–36.

842 22. Bergers G, Song S. The role of pericytes in blood-vessel formation and maintenance. Neuro-Oncol.
843 2005 Oct;7(4):452–64.

844 23. Duman RS, Monteggia LM. A neurotrophic model for stress-related mood disorders. Biol
845 Psychiatry. 2006 Jun 15;59(12):1116–27.

846 24. Doss JF, Corcoran DL, Jima DD, Telen MJ, Dave SS, Chi J-T. A comprehensive joint analysis of
847 the long and short RNA transcriptomes of human erythrocytes. BMC Genomics. 2015;16(1):952.

848 25. Hawrylycz MJ, Lein ES, Guillozet-Bongaarts AL, Shen EH, Ng L, Miller JA, et al. An anatomically
849 comprehensive atlas of the adult human brain transcriptome. Nature. 2012 Sep 20;489(7416):391–9.

850 26. Allen Brain Atlas. Technical White Paper: Case qualification and donor profiles, v.7 [Internet].
851 2013. Available from: help.brain-map.org

852 27. Allen Brain Atlas. Technical White Paper: Microarray Survey, v.7 [Internet]. 2013. Available from:
853 help.brain-map.org

854 28. Li JZ, Vawter MP, Walsh DM, Tomita H, Evans SJ, Choudary PV, et al. Systematic changes in
855 gene expression in postmortem human brains associated with tissue pH and terminal medical
856 conditions. Hum Mol Genet. 2004 Mar 15;13(6):609–16.

857 29. Tomita H, Vawter MP, Walsh DM, Evans SJ, Choudary PV, Li J, et al. Effect of agonal and
858 postmortem factors on gene expression profile: quality control in microarray analyses of
859 postmortem human brain. Biol Psychiatry. 2004 Feb 15;55(4):346–52.

860 30. Lanz TA, Joshi JJ, Reinhart V, Johnson K, Grantham LE, Volfson D. STEP levels are unchanged in
861 pre-frontal cortex and associative striatum in post-mortem human brain samples from subjects with
862 schizophrenia, bipolar disorder and major depressive disorder. PloS One. 2015;10(3):e0121744.

863 31. Barnes MR, Huxley-Jones J, Maycox PR, Lennon M, Thornber A, Kelly F, et al. Transcription and
864 pathway analysis of the superior temporal cortex and anterior prefrontal cortex in schizophrenia. J
865 Neurosci Res. 2011 Aug;89(8):1218–27.

866 32. Narayan S, Tang B, Head SR, Gilmartin TJ, Sutcliffe JG, Dean B, et al. Molecular profiles of
867 schizophrenia in the CNS at different stages of illness. Brain Res. 2008 Nov 6;1239:235–48.

868 33. Fasold M, Binder H. AffyRNADegradation: control and correction of RNA quality effects in
869 GeneChip expression data. Bioinformatics. 2013 Jan;29(1):129–31.

870 34. Fromer M, Roussos P, Sieberts SK, Johnson JS, Kavanagh DH, Perumal TM, et al. Gene expression
871 elucidates functional impact of polygenic risk for schizophrenia. Nat Neurosci. 2016
872 Nov;19(11):1442–53.

873 35. Viechtbauer W. Conducting Meta-Analyses in R with The metafor Package. J Stat Softw. 2010 Aug
874 1;36.

875 36. Pollard KS, Dudoit S, Laan MJ van der. Multiple Testing Procedures: the multtest Package and
876 Applications to Genomics. In: Bioinformatics and Computational Biology Solutions Using R and
877 Bioconductor [Internet]. Springer, New York, NY; 2005 [cited 2017 Oct 13]. p. 249–71. (Statistics
878 for Biology and Health). Available from: https://link.springer.com/chapter/10.1007/0-387-29362-
879 0_15

880 37. Huang DW, Sherman BT, Zheng X, Yang J, Imamichi T, Stephens R, et al. Extracting biological
881 meaning from large gene lists with DAVID. Curr Protoc Bioinforma Ed Board Andreas Baxevanis
882 Al. 2009 Sep;Chapter 13:Unit 13.11.

883 38. Huang DW, Sherman BT, Lempicki RA. Systematic and integrative analysis of large gene lists
884 using DAVID bioinformatics resources. Nat Protoc. 2009;4(1):44–57.

885 39. Subramanian A, Tamayo P, Mootha VK, Mukherjee S, Ebert BL, Gillette MA, et al. Gene set
886 enrichment analysis: a knowledge-based approach for interpreting genome-wide expression profiles.
887 Proc Natl Acad Sci U S A. 2005 Oct 25;102(43):15545–50.

888 40. Mootha VK, Lindgren CM, Eriksson K-F, Subramanian A, Sihag S, Lehar J, et al. PGC-1alpha-
889 responsive genes involved in oxidative phosphorylation are coordinately downregulated in human
890 diabetes. Nat Genet. 2003 Jul;34(3):267–73.

891 41. Sergushichev A. An algorithm for fast preranked gene set enrichment analysis using cumulative
892 statistic calculation. bioRxiv [Internet]. 2016 Jun 20; Available from:
893 http://biorxiv.org/content/early/2016/06/20/060012.abstract

894 42. Carpenter MB. Core Text of Neuroanatomy. 4th ed. Baltimore, MD: Williams & Wilkins; 1991.

895 43. Amaral DG, Scharfman HE, Lavenex P. The dentate gyrus: fundamental neuroanatomical
896 organization (dentate gyrus for dummies). Prog Brain Res. 2007;163:3–22.

897 44. Sun N, Cassell MD. Intrinsic GABAergic neurons in the rat central extended amygdala. J Comp
898 Neurol. 1993 Apr 15;330(3):381–404.

899 45. Li L, Welser JV, Dore-Duffy P, del Zoppo GJ, Lamanna JC, Milner R. In the hypoxic central
900 nervous system, endothelial cell proliferation is followed by astrocyte activation, proliferation, and
901 increased expression of the alpha 6 beta 4 integrin and dystroglycan. Glia. 2010 Aug;58(10):1157–
902 67.

903 46. Banasiak KJ, Haddad GG. Hypoxia-induced apoptosis: effect of hypoxic severity and role of p53 in
904 neuronal cell death. Brain Res. 1998 Jun 29;797(2):295–304.

905 47. Sowell ER, Peterson BS, Thompson PM, Welcome SE, Henkenius AL, Toga AW. Mapping cortical
906 change across the human life span. Nat Neurosci. 2003 Mar;6(3):309–15.

907 48. Rajkowska G, Miguel-Hidalgo JJ, Wei J, Dilley G, Pittman SD, Meltzer HY, et al. Morphometric
908 evidence for neuronal and glial prefrontal cell pathology in major depression. Biol Psychiatry. 1999
909 May 1;45(9):1085–98.

910 49. Smith DE, Rapp PR, McKay HM, Roberts JA, Tuszynski MH. Memory impairment in aged
911 primates is associated with focal death of cortical neurons and atrophy of subcortical neurons. J
912 Neurosci Off J Soc Neurosci. 2004 May 5;24(18):4373–81.

913 50. Stranahan AM, Jiam NT, Spiegel AM, Gallagher M. Aging reduces total neuron number in the
914 dorsal component of the rodent prefrontal cortex. J Comp Neurol. 2012 Apr 15;520(6):1318–26.

915 51. Peters A, Sethares C. Oligodendrocytes, their progenitors and other neuroglial cells in the aging
916 primate cerebral cortex. Cereb Cortex N Y N 1991. 2004 Sep;14(9):995–1007.

917 52. Resnick SM, Pham DL, Kraut MA, Zonderman AB, Davatzikos C. Longitudinal magnetic
918 resonance imaging studies of older adults: a shrinking brain. J Neurosci Off J Soc Neurosci. 2003
919 Apr 15;23(8):3295–301.

920 53. Salat DH, Buckner RL, Snyder AZ, Greve DN, Desikan RSR, Busa E, et al. Thinning of the
921 cerebral cortex in aging. Cereb Cortex N Y N 1991. 2004 Jul;14(7):721–30.

922 54. Peters A, Sethares C, Moss MB. HOW THE PRIMATE FORNIX IS AFFECTED BY AGE. J
923 Comp Neurol. 2010 Oct 1;518(19):3962–80.

924 55. Shepherd TM, Flint JJ, Thelwall PE, Stanisz GJ, Mareci TH, Yachnis AT, et al. Postmortem interval
925 alters the water relaxation and diffusion properties of rat nervous tissue--implications for MRI
926 studies of human autopsy samples. NeuroImage. 2009 Feb 1;44(3):820–6.

927 56. Cotter DR, Pariante CM, Everall IP. Glial cell abnormalities in major psychiatric disorders: The
928 evidence and implications. Brain Res Bull. 2001 Jul 15;55(5):585–95.

929 57. Banasr M, Duman RS. Glial loss in the prefrontal cortex is sufficient to induce depressive-like
930 behaviors. Biol Psychiatry. 2008 Nov 15;64(10):863–70.

931 58. RAGLAND JD, YOON J, MINZENBERG MJ, CARTER CS. Neuroimaging of cognitive disability
932 in schizophrenia: Search for a pathophysiological mechanism. Int Rev Psychiatry Abingdon Engl.
933 2007 Aug;19(4):417–27.

934 59. Atz M, Walsh D, Cartagena P, Li J, Evans S, Choudary P, et al. Methodological considerations for
935 gene expression profiling of human brain. J Neurosci Methods. 2007 Jul 30;163(2):295–309.

936 60. Vawter MP, Tomita H, Meng F, Bolstad B, Li J, Evans S, et al. Mitochondrial-related gene
937 expression changes are sensitive to agonal-pH state: implications for brain disorders. Mol
938 Psychiatry. 2006 Jul;11(7):615, 663–79.

939 61. Sequeira PA, Martin MV, Vawter MP. The first decade and beyond of transcriptional profiling in
940 schizophrenia. Neurobiol Dis. 2012 Jan 1;45(1):23–36.

941 62. Li JZ, Bunney BG, Meng F, Hagenauer MH, Walsh DM, Vawter MP, et al. Circadian patterns of
942 gene expression in the human brain and disruption in major depressive disorder. Proc Natl Acad Sci
943 U S A. 2013 Jun 11;110(24):9950–5.

944 63. Weis S, Llenos IC, Dulay JR, Elashoff M, Martínez-Murillo F, Miller CL. Quality control for
945 microarray analysis of human brain samples: The impact of postmortem factors, RNA
946 characteristics, and histopathology. J Neurosci Methods. 2007 Sep 30;165(2):198–209.

947 64. Hamberger A, Hyden H. Inverse enzymatic changes in neurons and glia during increased function
948 and hypoxia. J Cell Biol. 1963 Mar;16:521–5.

949 65. Kato T, Murashita J, Kamiya A, Shioiri T, Kato N, Inubushi T. Decreased brain intracellular pH
950 measured by P-31-MRS in bipolar disorder: a confirmation in drug-free patients and correlation
951 with white matter hyperintensity. Eur Arch Psychiatry Clin Neurosci. 1998 Dec;248(6):301–6.

952 66. Hamakawa H, Murashita J, Yamada N, Inubushi T, Kato N, Kato T. Reduced intracellular pH in the
953 basal ganglia and whole brain measured by P-31-MRS in bipolar disorder. Psychiatry Clin
954 Neurosci. 2004 Feb;58(1):82–8.

955 67. Johnson CP, Follmer RL, Oguz I, Warren LA, Christensen GE, Fiedorowicz JG, et al. Brain
956 abnormalities in bipolar disorder detected by quantitative T1 rho mapping. Mol Psychiatry. 2015
957 Feb;20(2):201–6.

958 68. Chesler M, Kraig R. Intracellular Ph of Astrocytes Increases Rapidly with Cortical Stimulation. Am
959 J Physiol. 1987 Oct;253(4):R666–70.

960 69. Peters A, Sethares C, Luebke JI. Synapses are lost during aging in the primate prefrontal cortex.
961 Neuroscience. 2008 Apr 9;152(4):970–81.

962 70. Guidotti A, Auta J, Davis JM, Di-Giorgi-Gerevini V, Dwivedi Y, Grayson DR, et al. Decrease in
963 reelin and glutamic acid decarboxylase67 (GAD67) expression in schizophrenia and bipolar
964 disorder: a postmortem brain study. Arch Gen Psychiatry. 2000 Nov;57(11):1061–9.

965 71. Hashimoto T, Volk DW, Eggan SM, Mirnics K, Pierri JN, Sun Z, et al. Gene expression deficits in a
966 subclass of GABA neurons in the prefrontal cortex of subjects with schizophrenia. J Neurosci Off J
967 Soc Neurosci. 2003 Jul 16;23(15):6315–26.

968 72. Volk DW, Austin MC, Pierri JN, Sampson AR, Lewis DA. Decreased glutamic acid
969 decarboxylase67 messenger RNA expression in a subset of prefrontal cortical gamma-aminobutyric
970 acid neurons in subjects with schizophrenia. Arch Gen Psychiatry. 2000 Mar;57(3):237–45.

971 73. Morris HM, Hashimoto T, Lewis DA. Alterations in somatostatin mRNA expression in the
972 dorsolateral prefrontal cortex of subjects with schizophrenia or schizoaffective disorder. Cereb
973 Cortex N Y N 1991. 2008 Jul;18(7):1575–87.

974 74. Volk D, Austin M, Pierri J, Sampson A, Lewis D. GABA transporter-1 mRNA in the prefrontal
975 cortex in schizophrenia: decreased expression in a subset of neurons. Am J Psychiatry. 2001
976 Feb;158(2):256–65.

977 75. Pandey GN, Dwivedi Y, Rizavi HS, Ren X, Pandey SC, Pesold C, et al. Higher expression of
978 serotonin 5-HT(2A) receptors in the postmortem brains of teenage suicide victims. Am J Psychiatry.
979 2002 Mar;159(3):419–29.

980 76. Pietersen CY, Mauney SA, Kim SS, Passeri E, Lim MP, Rooney RJ, et al. Molecular profiles of
981 parvalbumin-immunoreactive neurons in the superior temporal cortex in schizophrenia. J
982 Neurogenet. 2014 Jun;28(1–2):70–85.

983 77. Mauney SA, Pietersen CY, Sonntag K-C, Woo T-UW. Differentiation of oligodendrocyte
984 precursors is impaired in the prefrontal cortex in schizophrenia. Schizophr Res. 2015 Dec;169(1–
985 3):374–80.

986 78. Mistry M, Gillis J, Pavlidis P. Genome-wide expression profiling of schizophrenia using a large
987 combined cohort. Mol Psychiatry. 2013 Feb;18(2):215–25.

988 79. Choi KH, Higgs BW, Wendland JR, Song J, McMahon FJ, Webster MJ. Gene expression and
989 genetic variation data implicate PCLO in bipolar disorder. Biol Psychiatry. 2011 Feb 15;69(4):353–
990 9.

991 80. Montaño CM, Irizarry RA, Kaufmann WE, Talbot K, Gur RE, Feinberg AP, et al. Measuring cell-
992 type specific differential methylation in human brain tissue. Genome Biol. 2013;14(8):R94.

993 81. Tasic B, Menon V, Nguyen TN, Kim TK, Jarsky T, Yao Z, et al. Adult mouse cortical cell
994 taxonomy revealed by single cell transcriptomics. Nat Neurosci. 2016 Feb;19(2):335–46.

995 82. Mancarci O, Toker L, Tripathy S, Li B, Rocco B, Sibille E, et al. NeuroExpresso: A cross-
996 laboratory database of brain cell-type expression profiles with applications to marker gene
997 identification and bulk brain tissue transcriptome interpretation. bioRxiv [Internet]. 2016 Nov 22;
998 Available from: http://biorxiv.org/content/biorxiv/early/2016/11/22/089219.full.pdf

999 83. Bowling K, Ramaker RC, Lasseigne BN, Hagenauer M, Hardigan A, Davis N, et al. Post-mortem
1000 molecular profiling of three psychiatric disorders reveals widespread dysregulation of cell-type
1001 associated transcripts and refined disease-related transcription changes. bioRxiv. 2016 Jun
1002 29;061416.

1003 84. Chase KA, Rosen C, Gin H, Bjorkquist O, Feiner B, Marvin R, et al. Metabolic and inflammatory
1004 genes in schizophrenia. Psychiatry Res. 2015 Jan 30;225(1–2):208–11.

1005 85. Medina A, Watson SJ, Bunney W, Myers RM, Schatzberg A, Barchas J, et al. Evidence for
1006 alterations of the glial syncytial function in major depressive disorder. J Psychiatr Res. 2016
1007 Jan;72:15–21.

1008 86. Turner CA, Watson SJ, Akil H. The fibroblast growth factor family: neuromodulation of affective
1009 behavior. Neuron. 2012 Oct 4;76(1):160–74.

1010
1011